



eCOMMONS

Loyola University Chicago
Loyola eCommons

Master's Theses

Theses and Dissertations

2016

A Bioluminescence Sensor of NLRP3 Inflammasome Activation

Michael Alexander Winek
Loyola University Chicago

Follow this and additional works at: https://ecommons.luc.edu/luc_theses

 Part of the [Molecular Biology Commons](#)

Recommended Citation

Winek, Michael Alexander, "A Bioluminescence Sensor of NLRP3 Inflammasome Activation" (2016).
Master's Theses. 3157.
https://ecommons.luc.edu/luc_theses/3157

This Thesis is brought to you for free and open access by the Theses and Dissertations at Loyola eCommons. It has been accepted for inclusion in Master's Theses by an authorized administrator of Loyola eCommons. For more information, please contact ecommons@luc.edu.



This work is licensed under a [Creative Commons Attribution-NonCommercial-No Derivative Works 3.0 License](#).
Copyright © 2016 Michael Alexander Winek

LOYOLA UNIVERSITY CHICAGO

A BIOLUMINESCENCE SENSOR
OF NLRP3 INFLAMMASOME ACTIVATION

A THESIS SUBMITTED TO
THE FACULTY OF THE GRADUATE SCHOOL
IN CANDIDACY FOR THE DEGREE OF
MASTERS OF SCIENCE

PROGRAM IN NEUROSCIENCE

BY
MICHAEL A. WINEK
CHICAGO, IL
MAY 2016

Copyright by Michael A. Winek, 2016
All rights reserved.

ACKNOWLEDGMENTS

I would like to thank my committee members Dr. Collins and Dr. Stubbs for demanding the most of me in both my coursework and thesis project. I would like to thank Dr. Campbell for serving as my mentor and guiding me through this process and his invaluable lessons along the way. I would especially like to thank Dr. Campbell for challenging me with developing an essay. I thank my family for their support throughout the years in good times and bad.

TABLE OF CONTENTS

ACKNOWLEDGMENTS.....	iii	
LIST OF TABLES.....	v	
LIST OF FIGURES.....	vi	
LIST OF ABBREVIATIONS.....	viii	
ABSTRACT.....	x	
CHAPTER ONE: INTRODUCTION		
Statement of the Problem.....	1	
Inflammation.....	4	
PAMP's/DAMP's.....	7	
The Inflammasome.....	9	
NLRP3 Inflammasome.....	15	
Caspases.....	21	
Caspase 1.....	23	
Luciferase.....	23	
Firefly Luciferase.....	25	
Circular Permutated Luciferase (pGLO).....	25	
CHAPTER TWO: MATERIALS AND METHODS		
Cell Lines and Reagents.....	29	
Cell Culture.....	29	
Molecular Cloning.....	29	
Lentiviral Vector Generation.....	33	
Transfection.....	35	
Luminescence Readings.....	36	
CHAPTER THREE: RESULTS		
Generation of Candidate Inflammasome, Caspase-1 Sensors – Molecular Cloning.....	37	
Generation of Candidate Cathepsin B Sensors – Molecular Cloning.....	42	
Detection of Inflammasome Activation in Live Cells.....	44	
Linker Optimization and Characterization.....	48	
Caspase-1 Consensus Sequence and pGLDEVD specificity probe.....	49	
Generation of pLVX, pAAV, pCAG viral vector constructs.....	41, 55-57	
Inflammasome Activation in HeLa stable cell line.....	54	
CHAPTER FOUR: DISCUSSION		58
BIBLIOGRAPHY.....	64	
VITA.....	71	

LIST OF TABLES

Table	Page
1. <i>Cells of the Innate Immune Response</i>	6
2. <i>NLRP3 Inflammasome Associated Diseases</i>	20
3. <i>Caspase Consensus Sequences</i>	22
4. <i>Primers for insertion into linker region of pGLO-Caspase-1 targets</i>	31
5. <i>Primers for insertion into linker region of pGLO-Cathepsin B targets</i>	32
6. <i>Primers used for PCR amplification of pGLO gene</i>	34
7. <i>Peptide linker region targets of Caspase-1</i>	46

LIST OF FIGURES

Figure	Page
1. <i>Innate immune response to generalized bacterial infection</i>	6
2. <i>DAMP'S and PAMP's lead to inflammasome Activation</i>	8
3. <i>Two step process to NLRP3 inflammasome Activation</i>	11
4. <i>The spiral inflammasome Formation</i>	11
5. <i>NLR inflammasome Component Proteins</i>	12
6. <i>NLRP3 inflammasome Regulation and Activation</i>	16
7. <i>Caspase zymogen and 3-Dimensional structures</i>	22
8. <i>Molecular mechanism of pGLO</i>	27
9. <i>pGloSensor-30F construct</i>	38
10. <i>Predicted DNA bands from diagnostic restriction digest of clones generated in Figure 11-16:</i>	39
11. <i>pGL18 diagnostic restriction digest</i>	39
12. <i>pGLC7C1 (top) and pGLPA (bottom) diagnostic restriction digest</i>	40
13. <i>pGLIL1B diagnostic restriction digest</i>	40
14. <i>pGC75, pIL1B5 diagnostic restriction digest</i>	41
15. <i>pGLOST, pGLPPCB, pGLBTG, pGLBNDP, diagnostic restriction digest</i>	42

16. <i>pGLBID, pGLBIN, pGLREN, diagnostic restriction digest</i>	43
17. <i>Generalized experimental schematic</i>	45
18. <i>Transient transfection screen of 4 Caspase-1 target constructs</i>	47
19. <i>Transient transfection screen of 5AA mutants</i>	49
20. <i>Transient transfection screen of additional Caspase-1 target constructs presented as fold induction over control values.</i>	50
21. <i>pLVXC7C1 diagnostic restriction digest</i>	51
22. <i>pLVXIL18 diagnostic restriction digest</i>	52
23. <i>HeLa stable cell line lipofectamine inflammasome transfection</i>	54
24. <i>pGL-AAVC7C1 diagnostic restriction digest</i>	55
25. <i>pCAG-C7C1 diagnostic restriction digest</i>	56
26. <i>pCAG-IL18 diagnostic restriction digest</i>	57
27. <i>pCAG-WEHD diagnostic restriction digest</i>	57

LIST OF ABBREVIATIONS

ASC	Apoptosis-associated speck-like protein containing a CARD
CARD	Caspase Activation and Recruitment Domain
CASP1	Caspase 1
CASP7	Caspase 7
CATHB	Cathepsin B
cpLUC	Circularly permuted Luciferase encoded by PGLO
FFL	Firefly Luciferase
FLICA	Fluorescent Labeled Inhibitor of Caspases
GLOS	GloSensor™ cAMP Reagent
INF	Inflammasome
IL-1 β	Interleukin 1-Beta
IL-18	Interleukin 18
kD	Kilodalton
NLRP3IN	NLRP3 Inflammasome
ORF	Open-Reading-Frame
RLU	Relative Light Units
pGLAAV	Plasmid with a pGLO gene controlled by an AAV promoter
pGLCAG	Plasmid with a pGLO gene controlled by an CAG promoter
pLVX	pLVX lentiviral vector
PARK1	Parkin 1
PCR	Polymerase Chain Reaction
PGLO	pGloSensor™ plasmid construct
PRO-1	Pro-Caspase 1
PYD	Pyrin Domain

pGLC7C1	pGloSensor™ construct with Caspase 7 target sequence insertion
pGL18	pGloSensor™ construct with IL18 target sequence insertion
pGL1β	pGloSensor™ construct with IL1 β target sequence insertion
pGLPA	pGloSensor™ construct with Parkin 1 target sequence insertion
pGLC75	pGloSensor™ construct with Caspase 7 5AA target sequence insertion
pGLWEHD	pGloSensor™ construct with WEHDG 5 AA sequence insertion
pGL1β5	pGloSensor™ construct with IL1β 5AA target sequence insertion
BID1	BH3 interacting-domain death agonist
BNDP	β -neoendorphin dynorphin preprotein aka Proenkephalin B precursor
OST	Osteocalcin
BTG	Thyroglobulin
PPCATHB	Prepro Cathepsin B
RENIN	Renin Precursor Protein

ABSTRACT

The innate immune system is many organisms first line of defense against pathogenic insult or tissue damage [1]. This defense strategy is intent on restoring homeostasis upon perturbation. Upon activation of the innate immune system in humans, an oligomeric protein complex termed the “Inflammasome” forms in myeloid cells [2]. The canonical output of activation of any subset of inflammasome is Caspase-1-mediated secretion of pro-inflammatory cytokines IL1 β and IL18 [3, 4]. Chronic or uncontrolled inflammasome activation is at the core of myriad economically burdening diseases [5-8]. In many of these diseases, endogenous factors chronically engage the innate immune system. To study these diseases in *in vivo*, over time as they progress, in a transgenic organism will segue into the development of next generation therapeutics. In this study we sought to utilize a modified Firefly Luciferase (pGLO) construct to measure Caspase-1, and thus, inflammasome activity. pGLO has been engineered to be catalytically activated in response to targeted cleavage by a protease [9]. We report that insertion of a short peptide sequence targeted by Caspase-1 into the linker region of a circularly permuted Firefly Luciferase (pGLO) has allowed us to quantitatively assess the level of inflammasome activation in live cells. A successful *in vitro* experiment demonstrating sensitive and specific quantification of Caspase-1 activity should lead to an *in vivo* mouse model for the study of inflammatory disease.

CHAPTER ONE

INTRODUCTION

Statement of the Problem

Auto-Inflammatory diseases (AID), Metabolic Syndromes including Obesity and Type 2 Diabetes, and more recently Neurodegenerative Diseases all share a common thread of chronic dysregulation of inflammation [4, 5, 10, 11]. Alzheimer's disease is known to afflict approximately 6% of people over the age of 65, a growing concern as longevity steadily increases [12]. A constant amongst these disorders and disease states is a disruption in homeostatic control of the processing and secretion of IL1 β , an inflammatory cytokine involved in innate immunity [4, 13]. The generalized "Inflammasome" refers to a collection of related oligomeric platforms for activating Caspase-1 [2, 3, 14]. Caspase-1 can in turn process pro-inflammatory cytokines such as pro-IL1 β into mature cytokines to coordinate the innate immune response. Studies suggest that inflammasomes normally form in response to exogenous pathogen associated molecular patterns (PAMPs), or more simply conserved molecular motifs recognized by a Pattern Recognition Receptor (PRR) [15]. Endogenous "pathogens" in the form of Danger Associated Molecular Patterns (DAMP's) can activate Pattern Recognition Receptors in chronic disease states [13]. Loss of regulation of the formation, activation, or resolution of the inflammasome through pathways only beginning to be elucidated will be targets of future therapeutic intervention.

Quantitatively measuring the efficacy of therapeutics via high throughput screens (HTS) or *in vivo* animal model will greatly increase the number of “hits” to be further advanced into clinical trials. Presently, inflammasome activity can be quantified in the research laboratory by assays such as Western blotting, ELISA, or FLICA (Fluorescent Labeled Inhibitor of Caspases) [16] [17, 18]. The cellular pathway classically targeted in developing inflammasome assays is the aforementioned proteolytic processing of Pro-IL1 β by active Caspase-1 [18]. Thus, measuring levels of mature, secreted IL1 β protein in a sample preparation via ELISA is a go-to method of quantifying inflammasome activity *in vitro* [17] [18].

Fluorescent proteins conjugated to short peptide sequences, which fluoresce upon cleavage by proteases such as Caspase-1 (FLICA), present an alternative to ELISA. Similar to ELISA and Western blotting, these assays only work *in vitro* and display a narrow dynamic range in sensitivity [19]. Researchers have long known the strength of *luminescence* assays is in their broad dynamic range and minimal levels of background noise when compared to *fluorescence* assays. [20]. This thesis describes the development of a novel assay able to quantify inflammasome activity utilizing a genetically encoded Firefly Luciferase derived protein (pGLO). The ability to sensitively assess inflammasome activity, first in a high-throughput *in vitro* setting and subsequently in an *in vivo* animal model utilizing a dual purposed assay will be possible with the advances documented in this thesis.

. The potential to assess inflammasome activity *in vivo* with this technique makes it a powerful alternative to present assays. The literature has suggested that discrepancies

exist between Caspase substrates *in vitro* and *in vivo* affirming the need for an *in vivo* inflammasome and thus Caspase-1 assay [21]. Firefly Luciferase (FFL) derived proteins have been engineered to serve as bioluminescence sensors for a variety of intracellular and extracellular interactions. Structurally, Firefly Luciferases (FFL) uniquely possess a linker region between an N and C terminal domain as compared to other bioluminescent proteins [22]. This presents the possibility of forward genetic engineering modifications to alter FFL functionality in response to various stimuli.

It has been demonstrated that modifications to the unstructured linker region of a circularly permuted Firefly Luciferase (pGLO) can result in the generation of a sensor for cAMP, rapamycin and protease cleavage [19, 23, 24]. Many proteins, including the entire human Caspase family are known to cleave substrates in an unstructured extended loop conformation [25]. We hypothesize that the insertion of a short amino acid sequence cleaved by active Caspase-1 into the linker region of a circularly permuted Firefly Luciferase (pGLO) will result in a luminescence based inflammasome sensor.

With the drawbacks of current inflammatory assays in mind, the objective was to develop a novel, genetically encoded bioluminescence sensor for inflammasome activity. This technology is broadly applicable to the study of established and emerging diseases with any component of inflammasome activation. Furthermore, this study describes the use of a technology (pGLO) with the potential to measure the activity of any protease.

Inflammation

Inflammation is a highly coordinated response to stimuli in the form of exogenous pathogen, physical trauma, or endogenous factors [1, 13]. The inflammatory response occurs at the level of tissue and is mediated by resident immune cells and migratory cells. Tissue resident mast cells and phagocytes; which include dendritic cells and macrophages are responsible for the initial response (**Figure 1**). These cells can secrete chemokines and cytokines into the environment to coordinate the recruitment of circulating and subsequently infiltrating leukocytes (**Figure 1**). Dendritic cells secrete IL-12 or Interferon-Alpha in addition to presenting antigen to T-cells; this links the innate and adaptive immune responses [28]. Macrophages secrete over 9 Interleukins, TNF α , and CXCL's mainly involved in mediating migration and entry of neutrophils, basophils, eosinophils in addition to lymphocytes; another link between innate and adaptive immune responses [29].

The coordinated inflammatory response consists of two components. The innate immune system initiates the broad response to a diverse range of stimuli with the intent of restoring homeostasis. If this is insufficient in resolving the insult, the higher order adaptive immune response unique to vertebrates is activated [30]. This thesis describes the development of a sensor for the inflammasome and thus need not focus on the latter adaptive immune response.

Innate Immune System:

Innate Immunity begins with the epithelial layer of tissue. Once the epithelial layer of tissue is breached, then the innate immune system is initiated [30]. Conserved pathogenic motifs (PAMP's) can be recognized by membrane bound TLR's and large families of intracellular receptors of mast cells and macrophages [1] (**Figure 1**).

Membrane bound receptors typically belong to the family of Toll-Like Receptors (TLR's) containing a Leucine Rich Repeat Domain (LRR) are the first to be engaged [15, 31]. Intracellular receptors, which may be membrane bound in some cases include the NLR family, IPAF/NAIP, and NOD in addition to newly discovered less characterized receptors such as Interferon-Inducible Protein, AIM2 [2, 15]. The NLR family of receptors, the focus of this thesis, may be engaged by a swathe of stimuli. (**Figure 2 and Figure 3**). These receptors are thought of as separate signaling entities, the former TLR engagement as "Step 1" and the latter NLR receptor engagement as "Step 2." Upon successful engagement of both steps the inflammasome is activated [14].

Step 1 "Priming" involves the engagement of membrane bound TLR's by a PAMP or DAMP (**Figure 3**). Priming is important for the upregulation of NF κ B-controlled expression of pro-inflammatory genes. The NF κ B-induced increase in copy number of proIL1 β and proIL18 transcripts has been documented and plays a role in Step 2 [13]. Step 2 is the activation of the inflammasome via signaling through an NLR family, IPAF/NAIP, or NOD receptor protein. This two- step process has been conserved to avoid unnecessary inflammasome activation, which is thought to be a detriment to health [14].

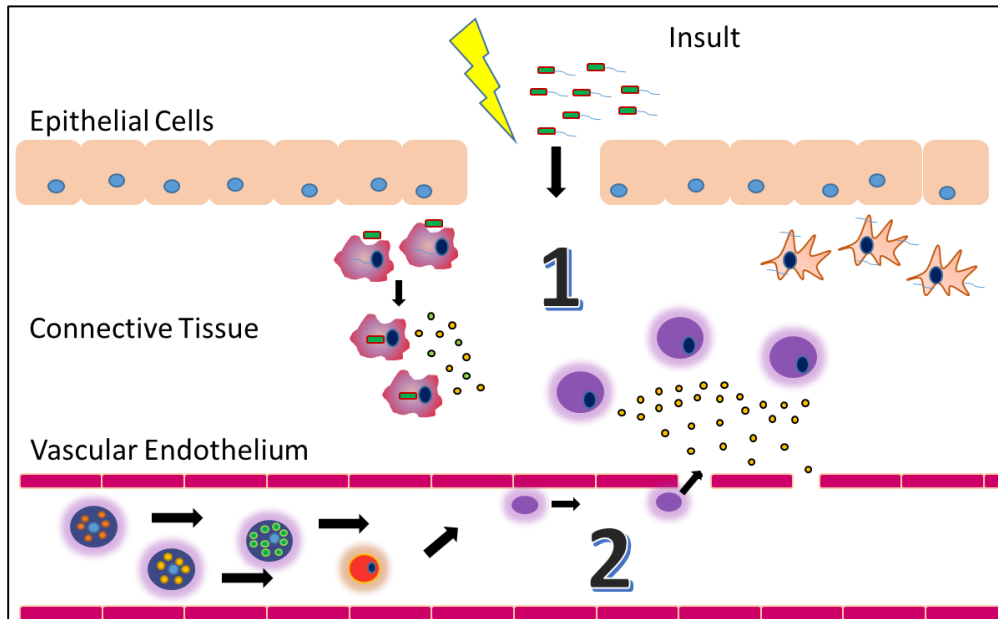


Figure 1: Innate Immune Response to generalized bacterial infection

1. Tissue Resident cells are the first responders and secrete chemokines and cytokines leading to (2)
2. Leukocytes migrate to the site of infection

Cell Type	Function	Location	Image
Mast Cell	Recruit Macrophages and Neutrophils, Dilate Blood Vessels, Release Histamine	Mucous Membranes Connective Tissue	
Macrophage	Phagocytosis, produce chemokines	All Tissues, can migrate	
Dendritic Cell	Antigen-presenting-cell (APC) initiating Adaptive Immunity	Epithelial tissue, migrates to lymph nodes	
Monocyte	Precursor to macrophages and dendritic cells, migratory	Spleen, migrates to site	
Eosinophil	Release toxic molecules (granules)	Circulating, migrates to site	
Basophil	Release Histamine, allergic reaction	Circulating, migrates to site	
Neutrophil	Most abundant, phagocytic, chemotactic, release granules	Circulating, migrates to site	

Table 1: Cells of the Innate Immune Response

(table adopted from [Boundless. "Pathogen Recognition." *Boundless Biology*. Boundless, 14 Sept. 2015.]])

PAMPS/DAMPS

PAMP's/DAMP's can activate different inflammasome subsets by signaling through both a TLR and subsequently the Leucine Rich Repeat (LRR) domain of a receptor (**Figure 2-3**). The LRR motif has been demonstrated to be involved in protein-protein interactions and has various mutations in TLR's allowing it them to recognize a diverse array of pathogens [31]. It is unclear at this point if the ligand activating the LRR is the PAMP/DAMP itself [14] [32]. Some suspect that unidentified intermediates may serve as the receptor for a PAMP/DAMP and signal through the LRR of the NLR inflammasome proteins. PAMP's are typically thought of as conserved motifs of DNA, RNA, or protein derived from a viral or bacterial infection recognized by a family of receptors yet to be described (**Figure 2**). Interestingly, the specific bacterial DNA motif thought to be recognized as a PAMP consists of a CpG motif comprising the dinucleotide CpG bordered by an upstream 5' purine pair and a downstream 3' purine pair [33]. Alternatively, and most important for this body of work, DAMP's are derived from the environment and have well-characterized disease associations listed and cited in **Table 2**. As indicated, **Table 2** illustrates disease associations for the best characterized NLRP3 inflammasome. Although, there may be a degree of cross-talk amongst inflammasome activation pathways leading to varying levels of activation of multiple species of inflammasome.

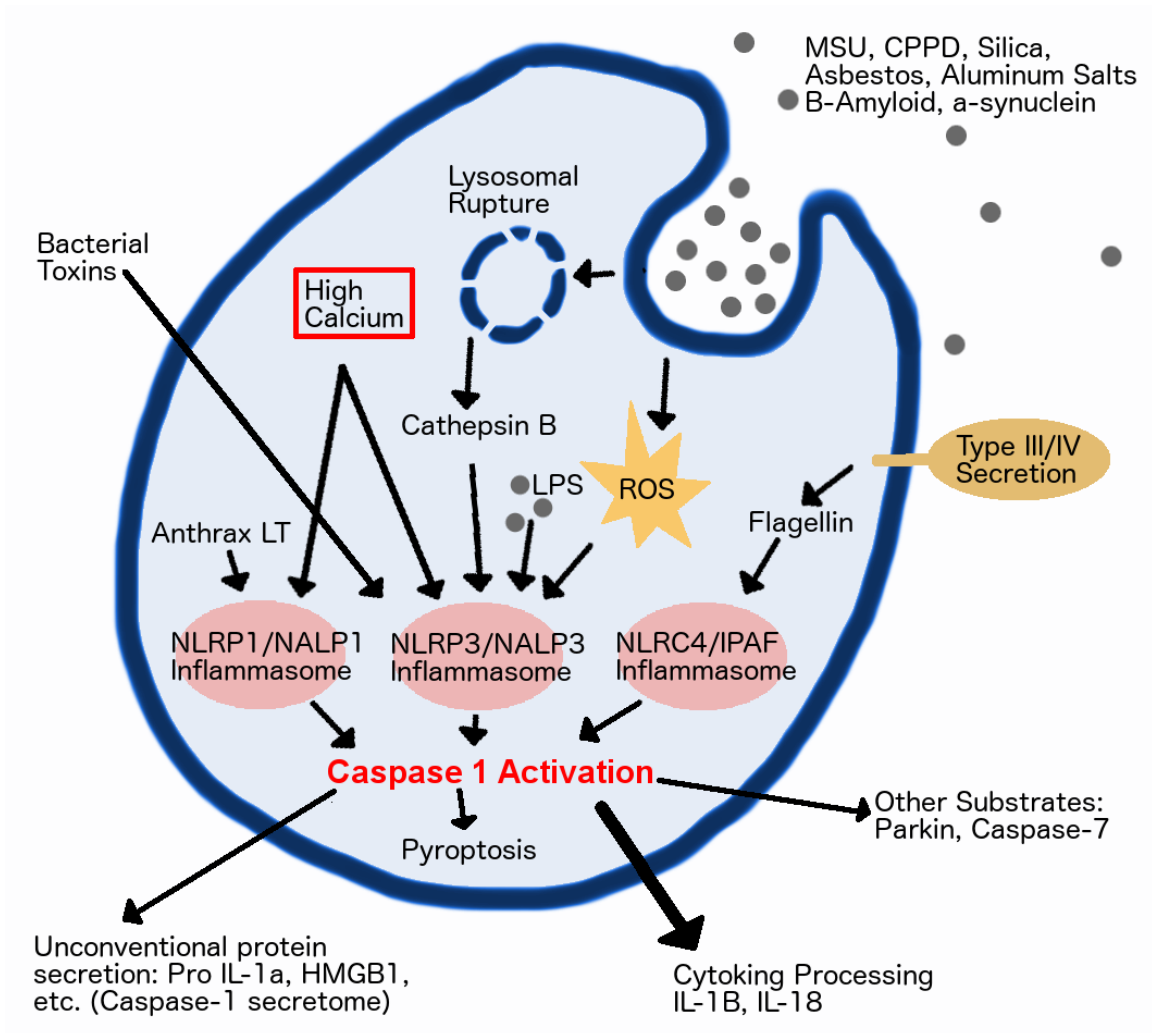


Figure 2: DAMP'S and PAMP'S lead to Inflammasome Activation
(Reproduced with permission of Margaret Bradley)

The Inflammasome

In 2002, Martinon et al, proposed the existence of a large oligomeric complex of proteins with the function to mediate immunity [3]. This is in light of the previous suggestion of a complex formed in cells on the pathway to apoptosis termed the “Apoptosome” [34]. This proposition has been affirmed with the discovery and ongoing discoveries of multiple subsets of inflammasomes [5, 13]. Inflammasomes have been shown to form in cells of the myeloid lineage, microglia, neurons, astrocytes, and keratinocytes [10, 14, 35] [14].

Upon the reception and activation of a primarily intracellular PRR, additional inflammasome components are recruited to the receptor. This is of course, preceded by Step 1, the priming step via TLR engagement by the PAMP or DAMP. **Figure 5** illustrates the general schematic and components of the best characterized inflammasomes. The common features to all inflammasomes is a receptor, sometimes an adaptor protein, ASC, and always Pro-Caspase-1 [36]. However, research suggests that Pro-Caspase-5 or perhaps Pro-Caspase-4 may take the place of Pro-Caspase-1 and play a role in active inflammasomes signaling [3]. The inflammasome components are thought to be self-oligomerizing [2]. It is known that assembly of the inflammasome is maintained through homotypic protein interactions often involving the adaptor protein ASC. CARD-CARD and PYRIN-PYRIN domain interactions of two proteins constituting the various species of inflammasomes hold the complex together [2]. It is speculated that the NLR receptor’s NACHT domain mediating receptor oligomerization is critical for formation of the inflammasome complex [37].

A diagram of the most extensively characterized inflammasome, NLRP3 can be seen in **Figure 3**. Presently it is unclear whether Pro-Caspase-1 or the Leucine Rich Repeat, (LRR) portion of an NLR lies on the inner portion of the complex [15]. The spiral-like oligomeric NLRP3 inflammasome complex is speculated to contain six or seven associated Receptor-Adaptor-Pro-Caspase-1 complexes [2] (**Figure 4**). As of now, it is unclear whether or not “heterocomplexes” of perhaps, an NLRP1 and NLRP3 inflammasome are formed [38] [39].

The common feature to all known inflammasome subsets is the processing of Pro-Caspase-1 into mature Caspase-1. Caspase-1 is an inflammatory protease classically known to cleave proIL1 β and proIL18 into their mature forms. Caspase-1 has 50-100 targets in humans with some overlap with proteins involved in apoptosis such as Caspase-7 [32]. Some have referred to the processes mediated by Caspase-1 as “pyroptosis,” a form of programmed cell death. Pyroptosis involves DNA cleavage, pore formation in the cell membrane, release of pro-inflammatory cytokines and subsequent cell death through swelling and lysis [40]. The pyroptotic process functions to limit the spread of a bacterial or viral infection [13].

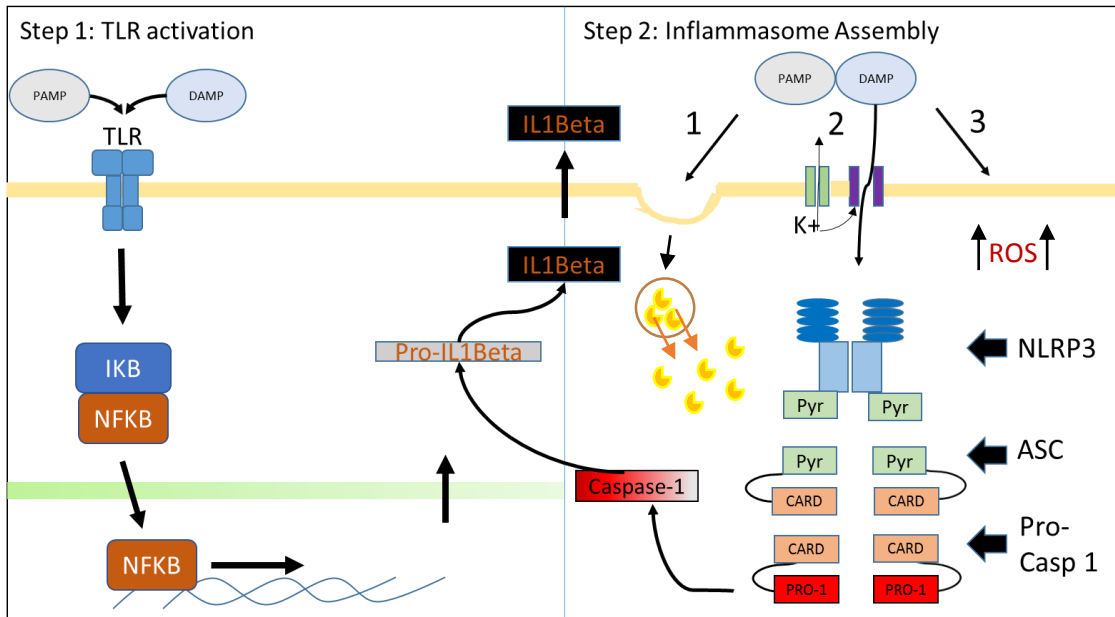


Figure 3: Two Step Process to NLRP3 Inflammasome Activation

Step 1: Priming a PAMP or DAMP described in *Table 5* induces NFκB transcription of pro-inflammatory cytokines. **Step 2: NLRP3 engagement** **1:** Endocytosis of a PAMP/DAMP leads to lysosomal leakage of Cathepsin B or ROS. **2:** K⁺ efflux triggers opening of Pannexin-1 allowing direct entry of PAMP/DAMP. **3:** Production of generalized ROS via PAMP/DAMP NLRP3 agonism activates the NLRP3 Inflammasome. (diagram adopted from [The Inflammasomes])

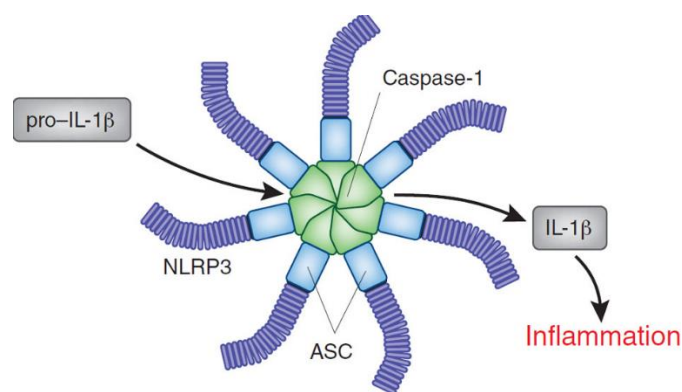


Figure 4: The Spiral Inflammasome Formation

(Permission granted through Rightslink®, (Klareskog and Hansson, 2011))

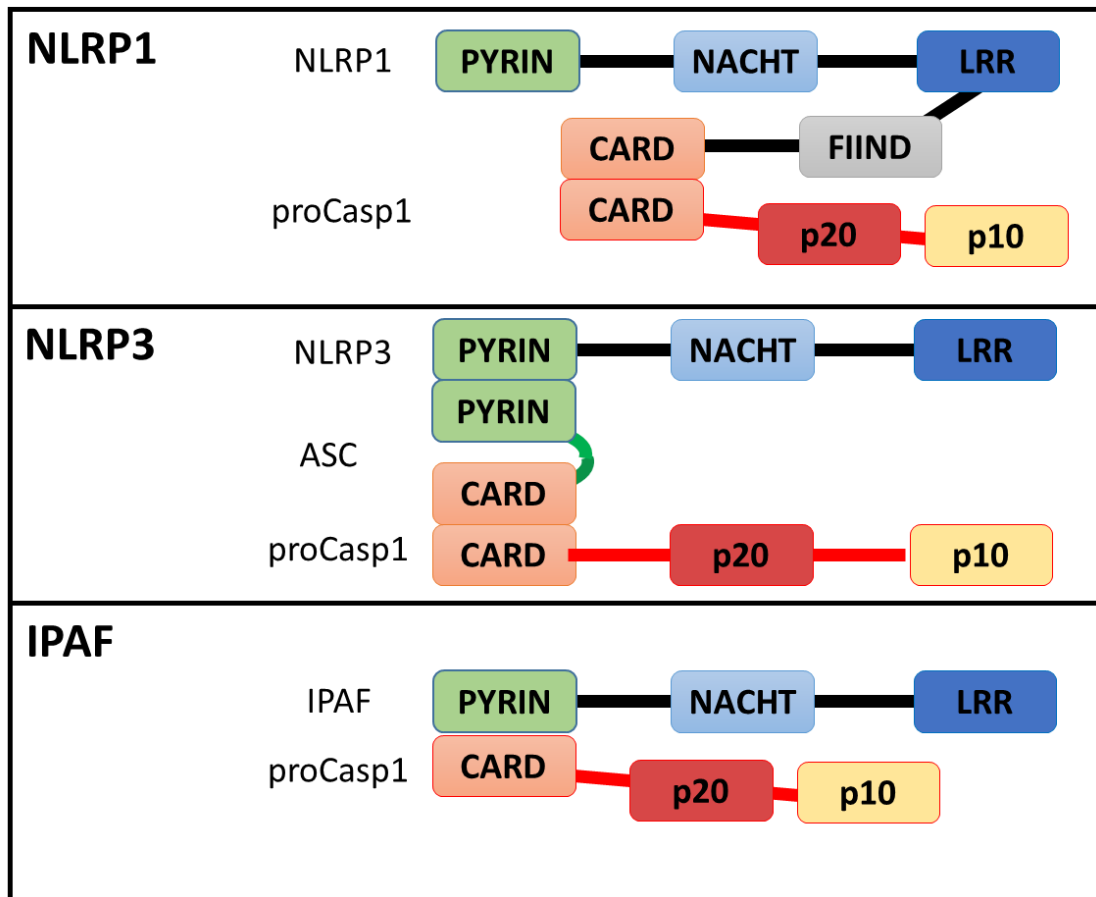


Figure 5: *NLR Inflammasome Component Proteins*

Abbreviations: PYRIN – Pyrin Domain, CARD – Caspase Activation and Recruitment Domain, LRR – Leucine Rich Repeat, FIIND – Function to Find Domain, p20 and p10 – large and small subunit of pro-Caspase-1, NACHT – Neuronal Apoptosis Inhibitor Protein

Regulation

The inflammasome and its immediate downstream processes are subject to transcriptional and post-translational regulation. The availability of the pro-IL1 β and pro-IL18 are under tight regulation via NF κ B signaling [15]. Whereas the expression of the adaptor ASC and Pro-Caspase-1 are found in many cell types; expression levels of the aforementioned PRR's are subject to variable cell type-specific expression patterns [4]. Factors such as the compartmental trafficking of inflammasome constituents, splice variants, microRNA, or existence of inhibitors can contribute to inflammasome regulation [41-43]. The inflammasome and IL1 β protein are similar in that they are subject to regulation through binding to decoy, dominant negative proteins [44] [41].

POP's

Little is known about inflammasome constituent trafficking or splice variants – particularly of the adaptor ASC [43]. However, a family of proteins referred to as Pyrin-Only-Proteins (POP's) , and CARD-Only-Proteins (COP's) have been documented to regulate inflammasome activity through direct homotypic interactions [45]. POP's are known to bind to the Pyrin domains of some NLR's and could perhaps bind to the Pyrin domain of the adaptor, ASC [41]. There are 2 POP's encoded in the human genome referred to as POP1 and POP2 with a very recently discovered POP3 [46]. A PAMP in the form of poxvirus have evolved an ability to suppress the host immune response in humans in response to their infection. This unique evolutionary strategy to evade innate immune surveillance is partially attributed to the presence of virally encoded POP's [47].

COP's

In humans COP's include Iceberg, COP1, INCA, Caspase-12 short (not present in some humans), and NOD2S [48]. Of the 5-protein family of COP's, a sequence similarity of between 53% to 92% with the CARD domain of Caspase-1 has been documented [49]. Genomically, COP's reside near the Inflammatory Caspases 1, 4, and 5 on human chromosome region 11q22.3 indicating evolution via gene duplication [49].

Adaptive Immune Regulation

Antigen-Presenting Cells (APC's) such as dendritic cells and macrophages also **(Figure 1)** phagocytose pathogens; which they display on their surface to migratory T-lymphocytes. T-lymphocytes are a broad class of cells consisting of Helper, Cytotoxic, Memory, Suppressor, and Natural Killer the function of which is related to their name and need not be detailed. As mentioned, APC mediated presentation of pathogenic antigen to T-Cells bridges the gap of innate and adaptive immunity. Type 1 Interferons a commonly utilized therapy in inflammatory disease, secreted by pathogen-infected cells play a role in decreasing inflammasome activity. ProIL1 protein can be decreased and Caspase-1 activation attenuated in Interferon- β -treated macrophages [50].

NLRP3 Inflammasome

As of late 2013, there were 274 NLRP3 inflammasome (NLRP3IN) related publications; by far the most extensively characterized subset of inflammasome. NLRP3IN is made up of NLRP3 receptor, ASC adaptor, and Pro-Caspase-1 [35]. The NLRP3 inflammasome was originally found to be activated by bacterial and viral toxins (PAMP's) such as Influenza, Sendai Virus, *Listeria Monocytogenes Staph Aureus*, and bacterial pore-forming toxins including Nigericin. Around 2008, researchers began to study the endogenous DAMP's found to chronically activate the NLRP3 inflammasome leading to the diseases found in (**Table 2**). There are 3 models of NLRP3 inflammasome activation proposed and thought to be the most substantiated by existing evidence (**Figure 3**) [2, 13].

1. **Endocytosis of PAMP's/DAMP's** leading to leakage of lysosomal proteases such as Cathepsin B into the cytosol [51] [52].
2. **K+ Efflux** Stimulation of P2X7 or P2X4 potassium (K+) ion channels via extracellular ATP. This triggers formation of large integral plasma membrane complexes-pannexins, which allow PAMP or DAMP entry and NLRP3 receptor engagement. Potassium efflux is highly implicated in this process with numerous studies aimed at elucidating the effects of varying intra versus extracellular potassium [53] [54].
3. **DAMP/PAMP induced increase in ROS.** The ROS sensitive Thioredoxin-Interacting Protein is a ligand for NLRP3 receptor and is thought to be involved. [55].

Research is beginning to implicate additional pathways of involvement with NLRP3 activation (**Figure 6**). These pathways are supported by minimal data but will serve as guidance for future directions in elucidating activation and regulation of *all* subsets of inflammasome. The utility of an inflammasome Sensor in further elucidating these pathways is significant.

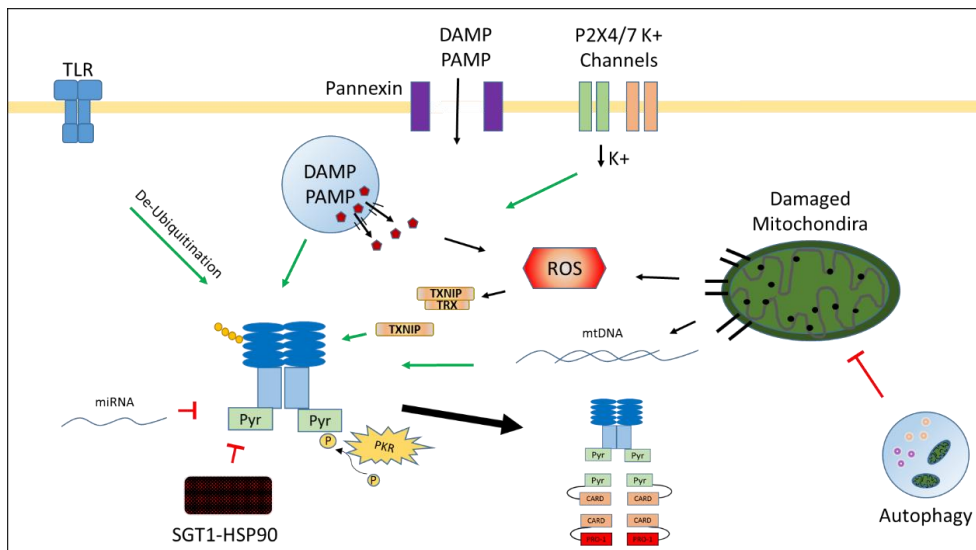


Figure 6: *NLRP3 Inflammasome Regulation and Activation* (permission granted through Rightslink®, diagram adopted from [56])

Green Arrow indicates Activation while Red indicates inhibition.

Additional NLRP3 activators

The role of additional molecular regulators of NLRP3 receptor activation and the formation of a complete NLRP3 inflammasome has received much attention. NLRP3 mRNA is under control of NF κ B and microRNA; as a result levels of the protein are variable amongst innate immune system cell types [57]. NLRP3 has been found to be ubiquitinated in a basal state; deubiquitination and activation were instigated by a priming signal. [58]. In mice, signaling through TLR4 relays through MyD88 coupled with mitochondrial ROS leading to deubiquitination of resting NLRP3 receptors [58]. It is speculated that multiple residues of NLRP3 are poly-ubiquitinated in a basal state and separate de-ubiquitinating enzymes activated by priming *or* activating signal lead to deubiquitination and activation. [58]. Protein Kinase R (PKR) directly interacts with NLRP3 and can regulate multiple inflammasome subsets [59]. A swathe of DAMP's including MSU, ATP, dsRNA, anthrax, and rotenone were able to induce a dampened inflammasome response when PKR is inhibited by genetic ablation or drug [59]. NLRP3 inhibition is thought to be mediated by LRR domains in addition to SGT1-HSP90 Chaperon complexes [60].

Reactive Oxygen Species (ROS) have been shown to play conflicting roles in NLRP3 inflammasome activation. Thioredoxin Interacting Protein (TXNIP) dissociates from Thioredoxin upon sensing ROS and like the above-mentioned regulators can bind to and activate NLRP3 [13]. The mitochondrial oxidative stress pathway has been implicated through interactions with autophagy, Ca⁺⁺ signaling, and ROS [61]. Autophagy, an intracellular degradation pathway, is responsible for digesting damaged

mitochondria. If this pathway is perturbed, then the effects of damaged mitochondria such as increased ROS and leakage of oxidized mtDNA induced by a PAMP/DAMP can lead to NLRP3 activation [62]. Strangely, Superoxide dismutase deficient-macrophages have elevated ROS, but display stunted inflammasome activity as shown by decreased cytokine production [63]. In these macrophages, Cys397 and Cys362 of Caspase-1 were found to be reversibly glutathionylated [63].

NLRP3 related Inflammatory Diseases

IL1 β and IL18 have been shown to be elevated in localized tissue or systemically throughout the body in an increasing number of diseases (**Table 2**). Drugs such as Kineret® (Anakinra) have been developed to broadly target the elevation of IL1 β through IL1 receptor antagonism. Future therapeutics will certainly offer more refined control of subsets of inflammasome rather than blanket modulation of the IL1R and in turn, IL1 β . Before these treatments make it to clinical trial, testing for safety and efficacy in an *in vivo* transgenic organism will decrease the cost of advancing the development of a therapeutic.

Cryopyrin-Associated Periodic Syndromes (CAPS)

Many rare auto-inflammatory diseases fall under a generalized category of: Cryopyrin-Associated Periodic Syndrome (CAPS). These are nearly all characterized by a mutated NLRP3 gene, increased NLRP3 inflammasome activity, and elevated IL1 β secretion. These orphan diseases are responsive to treatment with an Anakinra ®, an antagonist to the IL-1 receptor [5].

Neurodegenerative Disease

Alzheimer's disease, Parkinson's disease and Amyotrophic Lateral Sclerosis (ALS) all share a component of IL1 β elevation in the brain.[11, 64, 65] The protein aggregates formed by Amyloid- β ($\text{a}\beta$), α -synuclein, and SOD1 respectively are all thought to trigger activation of the NLRP3 or NLRP1 inflammasome as DAMP's. Microglia, thought of as very similar to myeloid cells are frequently found aggregated around these proteinaceous deposits/inclusion in Alzheimer's and Parkinson's disease. Microglia are essential for the inflammatory response in the CNS; however, neurons have been demonstrated to form NLRP1 inflammasomes as well. [4]

Metabolic Syndrome

The NLRP3 inflammasome has been demonstrated to be elevated in human individuals and mice fed a high-fat diet [13]. Broad spectrum IL1 receptor inhibition is being studied in clinical trials as a method of treating Type 2 Diabetes mediated by islet amyloid polypeptide (IAPP) activation of macrophages. [66-69]

Table 2: NLRP3 Inflammasome Associated Diseases

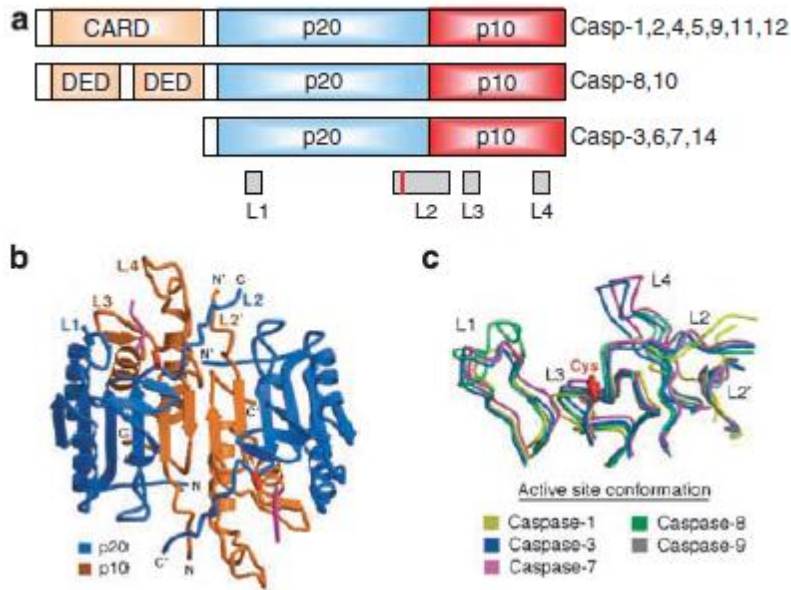
Disease	PAMP/DAMP	Cytokine	Reference
Gout	Uric Acid Crystals	IL1 β	7
Metabolic Syndromes	Ceramide, Free Fatty Acids	IL1 β	5, 66-69
Allergy	Islet Amyloid Polypeptide (IAPP) Hyaluronan, Dust Mites	IL18 IL1 β	4,5
Atherosclerosis	Cholesterol, Oxidized LDL	IL18	13, 35
Parkinson's	α -Synuclein	IL1 β	8,65
Alzheimer's	Amyloid- β	IL1 β	11,35,65
ALS	Super Oxide Dismutase 1	IL1 β	13

(Permission granted through Rightslink[®], table adopted from [5].)

Caspases

There are 11 Cysteine-Aspartate-Proteases in humans all of which normally exist in a pro-form (**Figure 7**) as approximately 30 to 53 kilodalton (kD) zymogens. The 11 human caspases are further classified into 3 distinct groups based on their functions, enzymatic preferences, and sequence homology. The two cleaved subunits from one pro-caspase can interact with two cleaved subunits from an identical pro-caspase to form an active tetrameric, mature caspase. It is currently unknown if p20 or p10 subunit from different pro-caspases can form chimeric, mature caspases. Caspases always cleave immediately after an aspartic acid residue in the P1 position. The 3 groups of caspases prefer different amino acid residues at other positions of their targets. The 3 positions preceding the P1 position are P2 preceded by P3 and then P4. The positions following P1 are typically referred to as, respectively, P1', P2', P3' etc. The P4 position is thought to be most important with regards to enzymatic specificity of caspase for their substrates; with the P2 and P3 positions playing much lesser roles [70].

In **Figure 7** one can see the similarities in the catalytic active site of a sampling of caspases from each group. Group 1 is Inflammation related, Group 2 is Apoptosis related, and Group 3 consists of upstream initiator caspases. Through generation of substrate libraries, the scientific literature has documented ideal, consensus cleavage sequences targeted by each caspase or group of caspases (**Table 4**). The Inflammatory caspases of Group 1 prefer the bulky hydrophobic amino acid tryptophan in the P4 position. The Apoptotic caspases of Group 2 prefer the more compact aspartate in P4 thus allowing for selectivity in this position due to exclusion of bulky amino acids.

Figure 7: Caspase zymogen and 3-Dimensional structure

(Permission granted through Rightslink®, [71])

Table 3: Caspase Consensus Sequences

Protein	Group	Optimal Sequence
Caspase-1	I	WEHD
Caspase-4	I	(W/L)EHD
Caspase-5	I	(W/L)EHD
Caspase-3	II	DEVD
Caspase-7	II	DEVD
Caspase-2	II	DEHD
Caspase-6	III	VEHD
Caspase-8	III	LETD
Caspase-9	III	LEHD

(Adopted from a table in [70])

Caspase 1

Caspase 1, previously known as Interleukin-1 β Converting Enzyme (ICE) is first synthesized as a 45kD pro-enzyme zymogen. Pro-Caspase-1 contains three distinct domains: CARD, p20, and p10 subunit domain. The Caspase-Activation and Recruitment Domain (CARD) is responsible for a homotypic interaction with a CARD domain of the adaptor ASC in the NLRP3 inflammasome. Upon activation of the inflammasome the p20 and p10 subunits are auto-proteolytically cleaved. Two p20 and two p10 subunits can associate to form a heterotetrameric active Caspase 1 enzyme.

The canonical output of Caspase 1 activation is the proteolytic processing of Pro-IL1 β and Pro-IL18 into their mature forms for secretion from innate immune cells of the myeloid lineage. This is of course proving to be true for other cell types more recently. Pro-IL1 β and pro-IL18 are the only Caspase-1 substrates found to be cleaved both *in vivo* and *in vitro* under pathological or physiological conditions [72].

Luciferase

“Luciferase” is a generic term referring to a class of enzymes with the function to catalyze a bioluminescent, light producing reaction in a variety of organisms. Reactions that catalyze bioluminescence with a “luciferase” type enzyme have evolved through convergent evolutions up to 30 times in both prokaryotes and eukaryotes [73]. The luciferase proteins receiving the most attention in biomedical research are Firefly Luciferase (*Photinus pyralis*), Renilla Luciferase (*Renilla Reniformis*), and Gaussia Luciferase (*Gaussia Princeps*) [74, 75]. Generally speaking, the catalytic mechanism in

producing light by all forms of luciferase involves an oxidation reaction of a type of luciferin molecule, resulting in the emission of a photon. Luciferases utilize a variety of cofactors in their light producing reactions including ATP, Ca⁺⁺, Riboflavin Phosphate, or O². As the molecular biology of Luciferase enzymes was beginning to be understood the potential to utilize these enzymes as reporters of fluctuations in cellular activity came to light.

The potential application of luciferase proteins in assays of genetic activity continues to be realized and advanced. In the beginning, people would place a luciferase gene downstream or otherwise under control of a candidate promoter and probe for the strength of the promoter. One could analyze normal or disease associated mutant promoter controlled gene expression via a downstream luciferase reporter. Most importantly, high-throughput screens (HTS) of candidate drug compounds could now be performed for targets of G-Protein Coupled Receptors (GPCR's) [20]. An example of this involves cloning a luciferase gene downstream and under control of a cAMP response element. Ultimately, a G-Protein Receptor activating drug will signal and converge on the increase in cAMP, it's binding to the CRE. The effect of the drug on signaling via this pathway or perhaps many others can be measured by bioluminescence proteins under genetic control CRE or another element.

Firefly Luciferase

Firefly Luciferase (FFL) is a 61kD monomeric enzyme with two distinct domains located towards the N and C termini separated by a linker [22]. Functionally, this linker region is thought to act as a molecular hinge between the two subunits. Catalytic activity is highest when the hinge motion is exercised through a “closed” conformation between the N and C terminal domains[22]. Firefly luciferase has continued to be utilized extensively as a reporter of intracellular activity since it was first cloned in 1985 [76]. In fact, as of 2010 ~21 percent of greater than 2000 assays listed on the PubChem database were bioluminescence based. [74] Firefly luciferase is ubiquitously used in research and development in the Dual Luciferase Assay popularized by Promega®. At the molecular level, Firefly Luciferase is normally free from post-translational modifications making it well-suited for a eukaryotic cellular environment of protein modifying enzymes. As the potential uses for FFL in HTS was continuing to be illustrated, people took considerable interest in modifying the protein through molecular biology for various applications. Researchers took to adding various intracellular localization sequences, degradation sequences, and even single nucleotide polymorphisms (SNP’s) to increase the catalytic efficiency of the enzyme [20, 74, 77].

Circularly Permutated Firefly Luciferase

Circular permutation of a protein is an alteration in the spatial order of amino acids in the overall primary peptide sequence. The protein may have a similar tertiary structure to the original protein yet the primary sequence is rearranged (**Figure 8, Left –**

Primary, Figure 8, Right– Tertiary). Circularly permuted proteins can be advantageous for researchers due to manipulation of factors such as thermostability, catalytic efficiency, and resistance to proteolytic processing [20, 77]. Through directed evolution by generation of large DNA libraries researchers can generate highly functional, novel, circularly permuted proteins [78, 79].

The early success of circularly permuted fluorescence based biosensors for intracellular events as early as 1999 may have corroborated the need for investment in the technology [78]. Promega® Corporation set out in the mid 2000's to evolve a circularly permuted Firefly Luciferase capable of monitoring intracellular events in real-time. This concept may have been influenced by the success of split luciferase technology which results in a fragmented protein engineered to reconstitute activity in response to an intracellular event [80] [81].

Directed evolution of a 544-AA protein began with the unstructured linker region between the N and C Terminus. The isolated mechanism of the N and C-terminal domains enclosing on the catalytic active site has been targeted in the design of cpLUC [22]. The design strategy involved the restriction of this enclosure mechanism via a modified hinge region [19]. Binkowski et al created a library of potential modified firefly luciferases tolerant of circular permutation, which they could test for functionality.

The first utility of cpLUC was discovered in sensing the activity of cAMP, rapamycin, and additional proteases. Researchers at the Promega® took to engineering restriction sites into the linker region of pGLO to allow for cut and paste cloning of short

amino acid (AA) sequences. First through overexpression studies, Promega® researchers tested the hypothesis that insertion of an AA sequence into the linker of cpLUC could lead to a sensor for protease activity. The hypothesis has proven true for developing pGLO based sensors of the proteases Caspase 3/7, Granzyme B, MERS CoV, TeV, [9, 19, 23, 24, 27, 82-84]

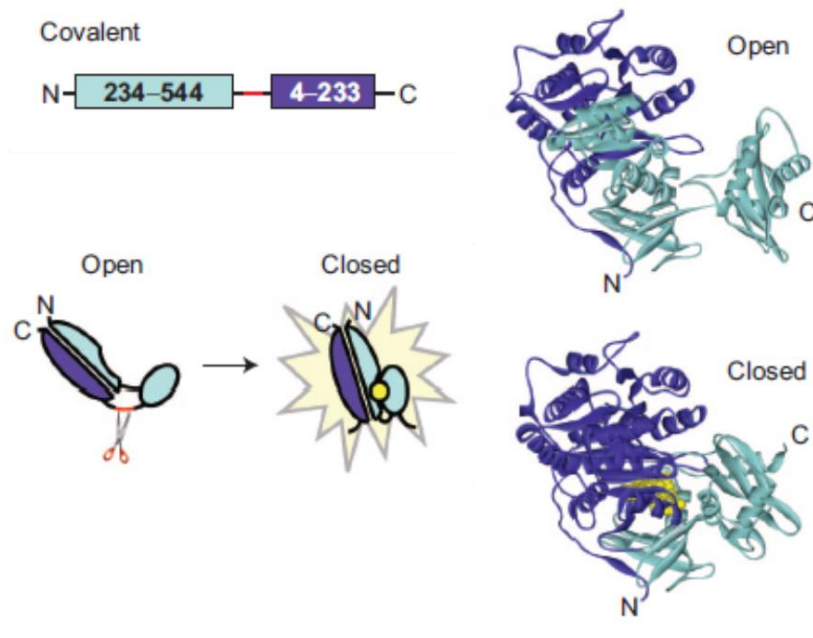


Figure 8: *Molecular Mechanism of pGLO*
(Reproduced with permission of Brock Binkowski, Promega® Corporation)

Hypotheses

We hypothesize that insertion of a Caspase 1 target sequence from a known substrate into a circularly permuted form of Firefly Luciferase (pGLO) will generate a sensitive and specific sensor for inflammasome activation

Specific Aim 1. To determine if we can detect Caspase-1 activation with our pGLO sensor construct

- A. Clone our Caspase 1 proteolytic target sequence into the pGLO modified luciferase sensor
- B. Overexpress two out of three components of the NLRP3 inflammasome and measure bioluminescence from live cells
- C. Create a stable cell line and measure bioluminescence in a physiologically relevant setting

CHAPTER TWO

MATERIALS AND METHODS

Cell Lines and Reagents

The human embryonic kidney cell line HEK293T and the human cervical epithelial cell line HeLa were obtained from the American Type Culture Collection (ATCC).

Cell Culture

HEK293T cells and HeLa cells were maintained in Dulbecco's Modified Eagle Medium (DMEM) media, supplemented with 10% fetal bovine serum (FBS), 100 IU/ml penicillin, 100 µg/ml streptomycin, 10 µg/mL ciprofloxacin. Cells were maintained in a 37° incubator with 5% CO².

Molecular Cloning

The pGloSensor-30F DEVDG (pGLO) construct was a kind gift from Promega® Corporation. Oligonucleotides for insertion into pGLO construct can be referenced in **Tables 3 and Table 4**. Primers were codon optimized for non-degeneracy via the reverse translation tool at www.bioinformatics.org. The pGLO construct was restriction digested overnight with BamH1 and Hind3 restriction enzymes in NEB buffer 3.1 both purchased from (New England Biolabs® Inc.) to reveal 2 overhang sites. Forward and Reverse primers from **Table 3** and **Table 4** were annealed via a PCR thermal cycler and ligated into the double digested pGLO construct using a Quick Ligation™ Kit (New England Biolabs® Inc.) Ligated constructs were transformed overnight with NEB 5-

alpha Competent *E.coli* (New England Biolabs® Inc) and selected for based on ampicillin resistance. Colonies were picked, grown up, and miniprep (QIAprep Spin Miniprep Kit, Qiagen®) following the manufacturer's instructions.

Diagnostic Restriction Digest

The pGLO sensor constructs in **Table 3** and **Table 4** were double digested overnight with SnaBI and HindIII restriction enzymes in NEB buffer 2.1 both purchased from (New England Biolabs® Inc.) The overnight digestion was mixed with 6x Loading Dye (New England Biolabs® Inc.) and 20 µl was loaded into each lane of a 1% agarose gel. 6 µl of Benchtop 1kB DNA Ladder (Promega®) was loaded into the first lane of each gel to visualize the size of each band. Gel electrophoresis was performed for ~45 minutes at 70V in 1X TAE buffer. Gels were visualized with a Chemi-Doc XRS+ (BioRad, Inc) using Image Lab Software. Putative DNA sequences for each sensor construct were digested utilizing the computer software program ApE (A Plasmid Editor) to determine predicted band size. Restriction digested clones can be referred to in **(Figures 10-16)** of the Results Section

Table 4: Primers for insertion into linker region of pGLO-Caspase 1 target:

Sequence	Primers 5' to 3' Fwd and Rev
pGLC7	gatccATTCAGGCGGATAGCGGCCCGATTGGa agcttCCAATCGGGCCGCTATCCGCCTGAATg
pGL18	gatccCTGGAAAGCGATTATTTTGGCAAAGGa agctTCCTTTGCCAAAATAATCGCTTTCCAGg
pGL1Beta	gatccTATGTGCATGATGCGCCGGTGCGCgga agctTCCGCGCACCGGCGCATCATGCACATAg
pGLPA	gatccCTGCATACCGATAGCCGCAAAGATGGa agctTCCATCTTTGCGGCTATCGGTATGCAGg
pGLC75	gatccCAGGCGGATAGCGGA agcttCCGCTATCCGCCTGg
pGLWE	gatccTGGGAACATGATGGa agctTCCATCATGTTCCCAg

Table 5: Primers for insertion into linker region of pGLO-Cath B Targets

Sequence	Primers 5' to 3' Fwd and Rev
pGLBID	gatccGCGAGCCGCAGCTTTAACCAGGGA agctTCCCTGGTTAAAGCTGCGGCTCGCG
pGLBIN	gatccGGCTTTGGCTTTGTGGGA agctTCCCACAAAGCCAAAGCCG
pGLBNDP	gatccGGCTTTCTGCGCCGCATTCGCCCA agctTGGGCGAATGCGGCGCAGAAAGCCG
pGLOST	gatccGCGTATCGCCGCTTTTATGGCCCA agctTGGGCCATAAAAAGCGGCGATACGCG
pGLBTG	gatccCCGACCGTGGGCAGCTTTGGCTTTGGA agctTCCAAAGCCAAAGCTGCCACGGTCGGG
pGLPPCB	gatccTATCTGAAACGCCTGTGCGGCACA agctTGTGCCGCACAGGCGTTTCAGATAG
pGLREN	gatccCCGATGAAACGCCTGACCCTGGGA agctTCCCAGGGTCAGGCGTTTCATCGGG

pLVX Lentiviral Vector

The best performing constructs (pGLC7C1 and pGL18) were selected to have the open reading frame (ORF) cloned into a lentiviral vector construct (pLVX). The pGLLVX primers in **Table 6** were designed to PCR amplify the gene of interest while inserting an Xho1 restriction site 5' and EcoR1 restriction site 3' immediately flanking the ORF of the pGLC7C1 or pGL18 gene. The pLVX construct was restriction digested overnight with Xho1 and EcoR1 restriction enzymes in NEB buffer 3.1 both purchased from (New England Biolabs ® Inc.) The amplified pGL18 and pGLC7C1 genes were ligated into the Multiple Cloning Site of the double digested pLVX plasmid construct using a Quick Ligation™ Kit (New England Biolabs ® Inc). Upon sequence verification the pLVX18 and pLVXC7 were transfected into HEK293T cells along with helper plasmids encoding VSVg and Capsid overnight. Media was changed on Day 1. On day 2 and day 3, supernatant was harvested, and filtered using a .45 micron filter. Supernatant containing pLVX viral vector (pLVX18 or pLVXC7C1) was stored at -80° C.

Table 6: Primers used for PCR amplification of pGLO gene

Sequence	Primers 5' to 3' Fwd and Rev
pGLLVX	ggccgCTCGAGcgccatgccgggatcaac cggccGAATTCttaaacacctttcggtgt
pGLAAV	ggccgGAATTCcgccatgccgggatcaac cggccCTCGAGttaaacacctttcggtgt
pGLCAG	ggccgGAATTCcgccatgccgggatcaac cggccCTCGAGttaaacacctttcggtgt

pGLAAV and pGLCAG Viral Vector

Of the best performing constructs (pGLC7C1, pGL18, and pGLWEHD), pGLC7C1 was selected to have the open reading frame of the pGLO protein cloned into an AAV vector construct (pGLAAV) and CAG promoter construct (pGLCAG). The pAAV and pGLCAG primers were designed to PCR amplify the ORF of our gene of interest while inserting an EcoR1 restriction site 5' and Xho1 restriction site 3' of the gene. The pGLAAV and pGLCAG constructs were restriction digested overnight with EcoR1 and Xho1 restriction enzymes in NEB buffer 3.1 both purchased from (New England Biolabs® Inc.) The amplified pGL18 and pGLC7C1 genes were ligated into the MCS of the pGLAAV and pGLCAG plasmids using a Quick Ligation™ Kit (New England Biolabs® Inc.). Upon sequence verification the pGLAAVC7, pGLCAGC7, pGLCAG18 and pCAGWE were stored at -20° C.

PEI Transfection

HEK293T cells were plated at ~70 percent confluence in 100 microliters (μ l) of DMEM per well of a 96 well black wall, clear bottom plate (Corning® Inc). Cells were allowed to adhere to the wells for 3 hours. In 41.5 μ l of oxidized DMEM 225 nanograms (ng) of a pGLO sensor construct for each of the target sequences in Table 1 with 75 ng of a construct expressing ASC and 75 ng of a construct expressing Pro-Caspase-1 were allowed to equilibrate for 5 minutes. Oxidized DMEM is prepared by leaving regular DMEM as described previously overnight at room temperature on a shaker for ~5 days. 1 μ l of vortexed polyethylenimine (PEI) was added to each 41.5 μ l tube and allowed to form liposome complexes for 10 minutes. 13 μ l of each 41.5 μ l pGLO sensor transfection tube was dropped onto 1 well of a 96 well plate in triplicate. Cells were incubated with PEI transfection complexes overnight for 14 hours and withdrawn the next day. Media was replaced with CO² independent media supplemented with 10% FBS (Life Technologies) only and allowed to equilibrate for 2 hours prior to addition of GloSensor® reagent (GLOS) (Promega®).

Lipofectamine 2000 Transfection

HeLa cells were plated in the afternoon at ~70 percent confluence in 100 μ l of DMEM per well of a 96 well black wall, clear bottom plate (Corning®) Cells were allowed to adhere to the wells for 3 hours. Transient transfection was performed according to the manufacturers protocol (Invitrogen®) with a final volume of .3 μ l Lipofectamine 2000 reagent and 100 ng of DNA per well. Experiments were performed

in triplicate. Cells were incubated with transfection complexes overnight for 14 hours and withdrawn the next day. Media was replaced with CO² independent media supplemented with 10% FBS only, and allowed to equilibrate for 2 hours prior to addition of GloSensor reagent (GLOS).

Luminometer Readings

GloSensor reagent (GLOS) lyophilized powder was reconstituted as per the manufacturer's protocol in 10mM HEPES at a pH of 7.5. 2 µl of GLOS was added directly to 100 µl of CO² independent media in each well of a 96 well plate and allowed to equilibrate for 2 hours. Readings were taken in a GloMax®-96 Microplate Luminometer (Promega) every hour for 3-5 hours. Luminometer settings were as follows for all reported experimental data collection: No injection, 1 Run, No Delay between runs with an integration time of 1 second.

CHAPTER THREE

RESULTS

Generation of Candidate Inflammasome, Caspase-1 Sensors – Molecular Cloning

The pGloSensor-30F (pGLO) plasmid construct encodes a circularly permuted Firefly Luciferase (cpLUC) with an unstructured linker region between N and C terminal domains (**Figure 9**.) This linker region is unstructured and has been modified by Promega® Corporation to contain two restriction sites, BamHI and HindIII. The restriction sites are unique to the construct such that digestion of both sites will yield a region where a short DNA sequence can be ligated. DNA encoding six separate amino acid sequences recognized and cleaved by Caspase-1 was ligated into the pGLO (**Table 7**). Data shown in **Figures 11-16** are diagnostic restriction digests to verify that the candidate linker sequence has been inserted into pGLO. Double digesting the unique linker region would yield an small approximately 20 base pair fragment unable to be resolved on a standard agarose gel. We identified two SnaB1 sites and one Hind3 site which upon overnight double digest with each enzyme would yield bands of approximately 3997, 2702, and 1178 base pairs in length. The 3 predicted fragments can be seen in **Figure 10**. Clones that upon double digestion with SnaB1 and Hind3 had bands matching those of **Figure 10** were sent for sequencing.

Upon correct Sanger sequencing verification; the screen for the best performing Caspase-1 sensor could be performed. Refer to **Table 4-5** in Materials and Methods for DNA sequence insertions for **Figures 11-16**.

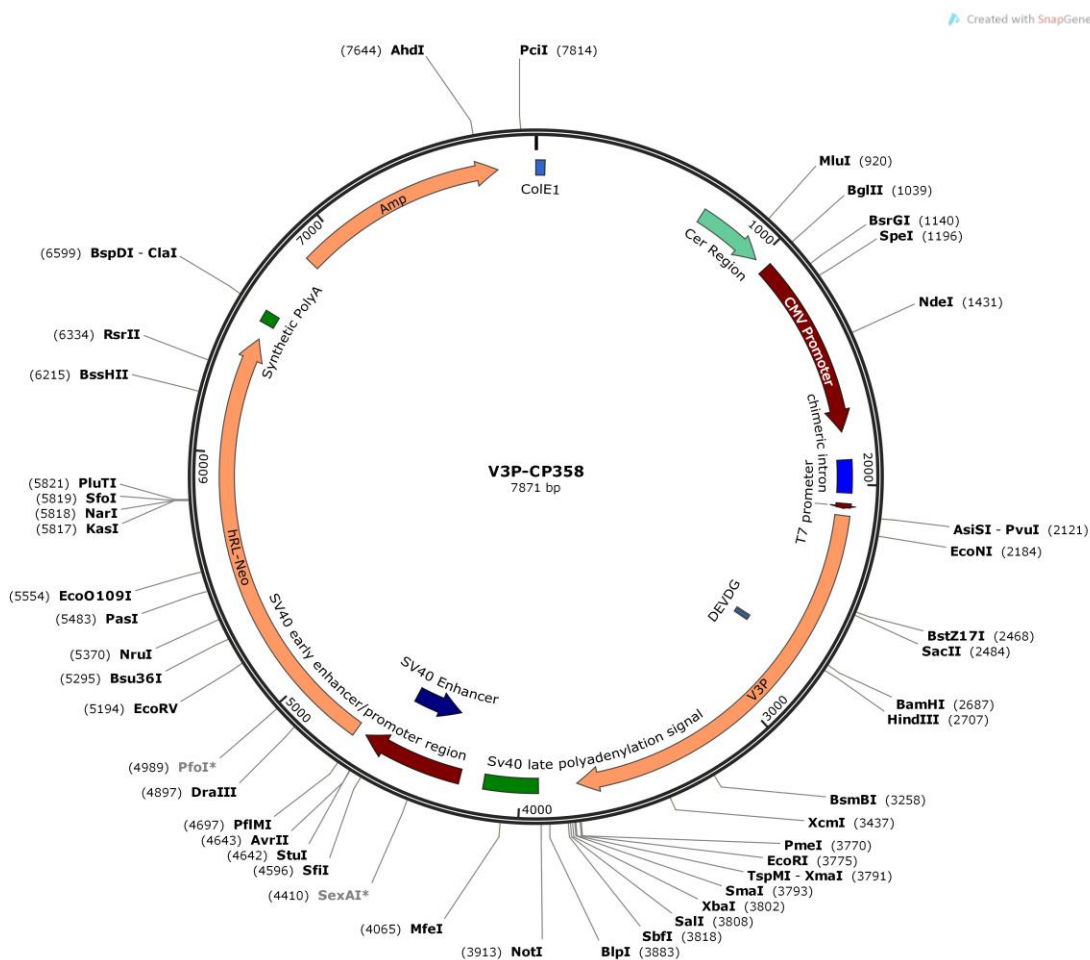


Figure 9: pGloSensor-30F construct

Image provided courtesy of SnapGene, www.snapgene.com

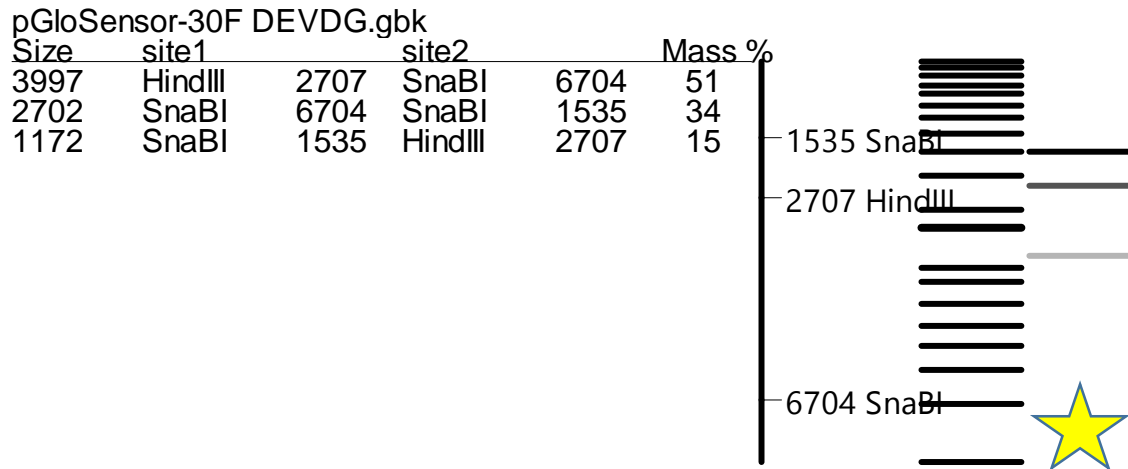


Figure 10: Predicted DNA bands from diagnostic restriction digest of clones generated in **Figure 11-16:**

Image is obtained from the software program ApE – A Plasmid Editor by M. Wayne Davis. Simulated DNA gel on the right indicates the size of bands one would expect upon restriction digest of the pGLO vector with SnaBI and HindIII with a properly inserted linker region. The proceeding figures are evidence of successful cloning as per the lanes indicated by a star which match the predicted lane in the above figure.

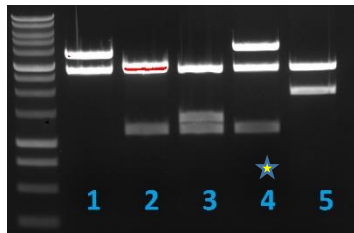


Figure 11: pGL18 diagnostic restriction digest
Lanes 1-5 pGL18 individual clones

Lanes marked with a star indicate a positive clone as verified by diagnostic digest by SnaBI and HindIII matching predicted bands in **Figure 10** as well as Sanger Sequencing verification



Figure 12: *pGLC7C1* and *pGLPA* diagnostic restriction digest
Lanes 1-5 *pGLC7C1* individual clones, Lanes 6-9 *pGLPA* clones

Lanes marked with a star indicate a positive clone as verified by diagnostic digest by *Sna*B1 and *Hind*III matching predicted bands in **Figure 10** as well as Sanger Sequencing verification

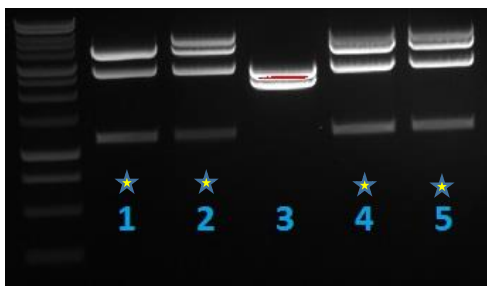


Figure 13: *pGLIL1β* diagnostic restriction digest
Lanes 1-5 *pGLIL1β* individual clones

Lanes marked with a star indicate a positive clone as verified by diagnostic digest by *Sna*B1 and *Hind*III matching predicted bands in **Figure 10** as well as Sanger Sequencing verification

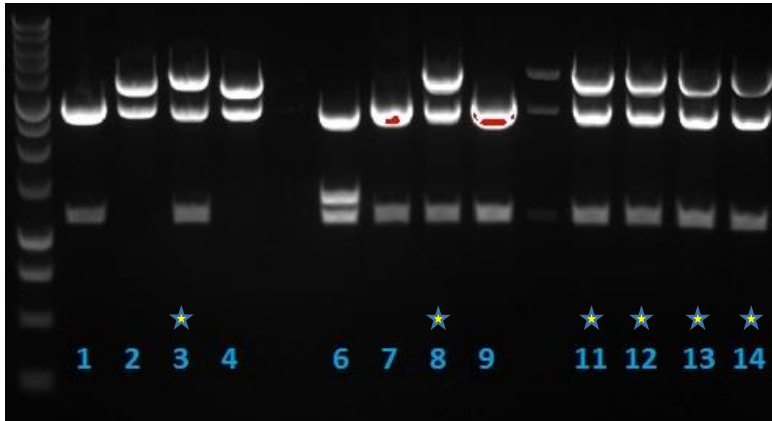


Figure 14: *pGC75, pL165 diagnostic restriction digest*

Lanes 1-4 pGLC75 individual clones, Lanes 6-14 pGLIL1β5 individual clones

Lanes marked with a star indicate a positive clone as verified by diagnostic digest by SnaB1 and HindIII matching predicted bands in **Figure 10** as well as Sanger Sequencing verification

Generation of Candidate Cathepsin B Sensors – Molecular Cloning

DNA encoding six separate amino acid sequences recognized and cleaved by Cathepsin B were ligated into pGLO. As per the generation of the Caspase-1 sensors, two *Sna*B1 sites and one *Hind*3 site were identified which upon overnight double digestion with each enzyme would yield bands of approximately 3997, 2702, and 1178 base pairs in length. The 3 predicted fragments can be seen in **Figure 15-16**. The data shown in **Figure 15-16** is diagnostic restriction digest to verify that the candidate linker sequence has been inserted into the pGLO

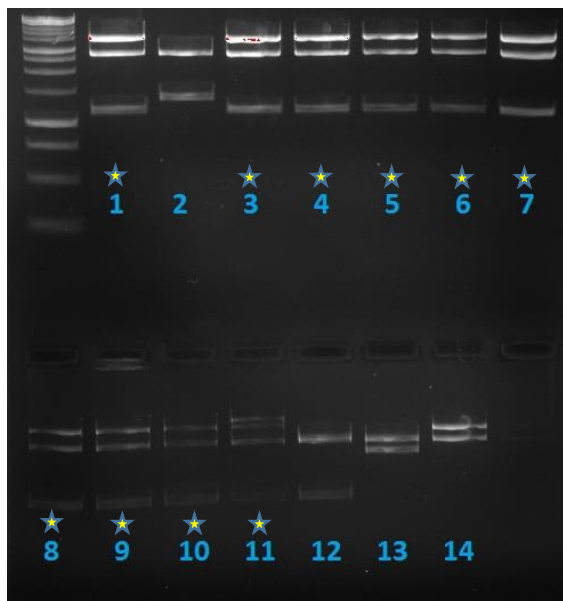


Figure 15: *pGLOST, pGLPPCB, pGLBTG, pGLBNDP, diagnostic restriction digest*

Lanes 1-4 *pGLOST*, 5-8 *pGLPPCB*, 9-11 *pGLBTG*, 12-14 *pGLBNDP* individual clones

Lanes marked with a star indicate a positive clone as verified by diagnostic digest by *Sna*B1 and *Hind*III matching predicted bands in **Figure 10** as well as Sanger Sequencing verification

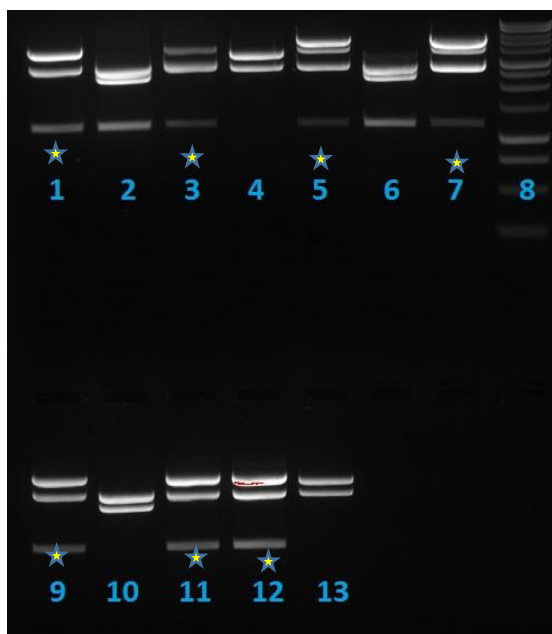


Figure 16: *pGLBID, pGLBIN, pGLREN, diagnostic restriction digest*
Lanes 1-4 pGLBID, 5-7, 9 pGLBIN, 10-13 pGLREN individual clones

Lanes marked with a star indicate a positive clone as verified by diagnostic digest by *SnaB1* and *HindIII* matching predicted bands in **Figure 10** as well as Sanger Sequencing verification

Detection of Inflammasome Activation in Live Cells

The pGloSensor™ (pGLO) construct encodes a luciferase protein (cpLUC) from *Photuris pensylvanica* with a similar catalytic mechanism to commonly utilized firefly, *Photinus pyralis* luciferase. cpLUC has been circularly permuted at residue 358 such that amino acid residues 358-544 are now positioned towards the N-Terminus and 4-354 are at the C-Terminus with an unstructured Gly-Ser linker region in between. **(Figure 8)** It has been demonstrated that by inserting in certain consensus cleavage sequences targeted by specific proteases one can observe statistically significant increases in luminescence upon activation of the respective protease. The pGLO construct we began our studies with has been optimized for detecting Caspase 3/7 activity through cleavage of a 5 amino acid DEVDG linker region. pGLDEVD has undergone a high throughput screen (HTS) of over 21,648 possible mutations for the best performing construct [27]. The optimized pGLDEVD for detection of Caspase 3/7 activation has a Threonine to Isoleucine point mutation at amino acid 151 as compared to the pGloSensor22F construct available commercially through Promega®.

There are a small number of publications utilizing the generalized pGLO construct to measure protease activity for proteins such as: Granzyme B, Caspase 3/7, and MERS CoV papain like protease. We initially choose to screen four 8 amino acid sequences from the proteins IL1 β , IL18, Parkin1, and Caspase 7 [85-88]. To probe for the sensitivity of the constructs designed for our screen we transiently transfected HEK293T cells with a plasmid encoding one construct from: pGLIL1 β , pGL18, pGLPA, and pGLC7C1. To activate the Inflammasome in a non-myeloid cell line presumed to

not exhibit capabilities for induction of robust Caspase-1 activity; we co-transfected two of the three components of the NLRP3 Inflammasome, ASC and Pro-Caspase 1.

HEK293T cells were transfected, in triplicate, overnight and luminescence measured 14 hours post transfection in a 96 well plate (**Figure 17**). Each experimental well (XP) of a 96 well plate received 75ng pGLO candidate sensor, 25ng ASC, and 25ng Pro1. The control wells (CTRL) substituted ASC and Pro1 for 50 ng of GFP. To our surprise, pGLC7C1 cleavage resulted in the highest levels of luminescence in both raw RLU as well as fold induction versus GFP control as seen in (**Figure 18**). Our initial hypothesis favored pGLIL1 β , containing a cleavage sequence recognized by the literature as belonging to the canonical output of inflammasome activation as the front-runner for the candidacy as the most robust inflammasome sensor.

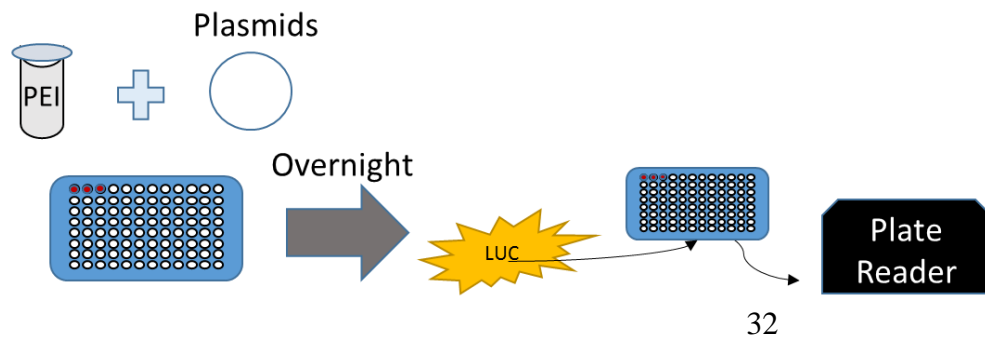


Figure 17: *Generalized Experimental Schematic*

Table 7: Peptide linker region targets of Caspase-1

Sequence	Peptide Linker	Reference
pGLC7C1	IQAD-SGPIG	86,89
pGLIL1 β	YVHD-APVRG	87
pGL18	LESD-YFGKG	88
pGLPA	LHTD-SRKDG	85
pGLC75	QAD-SG	86,89
pGLWEHD	WEHD-G	70

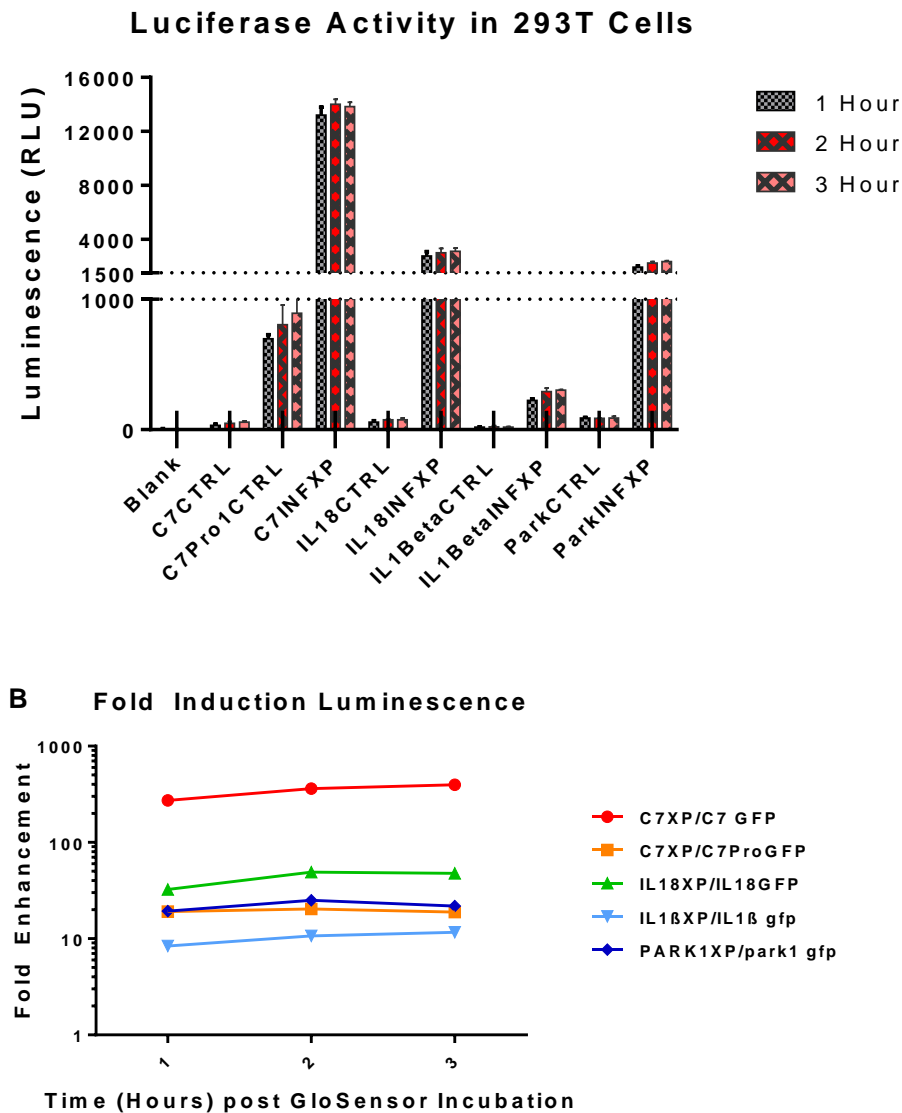


Figure 18: Transient Transfection screen of 4 Caspase 1 target constructs

(A) Luminometer data from PEI transfection of HEK293T cells at various time points post GloSensor (GLOS) incubation. Each control wells (CTRL) received 75ng pGLO candidate sensor, 50ng GFP. Each experimental wells (XP) received 75ng pGLO candidate sensor, 25ng ASC, 25ng Pro-Caspase-1. Data represent the mean and standard deviation of 3 replicates.

(B) Fold induction luminescence of experimental well versus control. Values are calculated by dividing pGLO candidate XP value by pGLO candidate CTRL value at each indicated time point. Data represent the mean of 3 replicates.

Fold Induction Inflammasome Activation

To standardize for the various types of luminometers (LUM) commercially available, luminescence data is typically presented as fold induction versus control. **(Figure 18)** The numerator in the calculation for fold induction is the raw value in RLU for a given candidate sensor construct with co-transfection of ASC and Pro-Caspase-1. The denominator in the calculation is the raw value in RLU for a given candidate sensor construct with co-transfection of equalized volume of GFP.

Linker Optimization and Characterization

cpLUC has undergone molecular changes especially in its DNA sequence but also to a lesser degree in its overall tertiary and quaternary structure. The catalytic activity of the protein is indeed intact, however, it is a hypo-functional enzyme compared to wild type FFL. As the success of the original Caspase 3/7 sensor, pGLDEVD involved a 5 amino acid linker region instead of 8; we hypothesized that reducing the length of the linker region in our most robust sensor may increase the sensitivity. We removed 4 amino acids, from a linker region which was previously 8 amino acids in the construct generating the highest levels of luminescence. We performed the same experimental paradigm as in **Figure 17** by co-expressing ASC and Pro-Caspase-1 together with one of two candidate sensors in HEK293T cells. The data suggest that in our screen for Caspase 1 cleavage sequences, an 8 amino acid target sequence is ideal versus a truncated form of the same sequence.

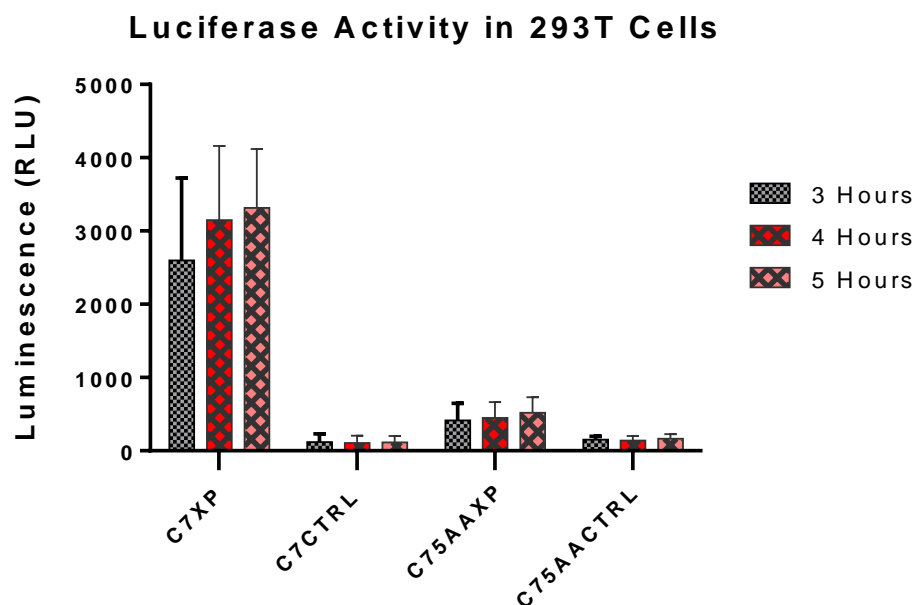


Figure 19: Transient Transfection Screen of 5AA mutants

Luminometer data from PEI transfection of HEK293T cells. Each control wells (C7CTRL or C75AACTRL) received 75ng pGLO candidate sensor pGLC7C1 or pGLC7C5, 50ng GFP. Each experimental wells (XP) received 75ng pGLO candidate sensor (pGLC7C1 or pGLC7C5), 25 ng ASC, 25 ng Pro-Caspase-1. Data represent the mean and standard deviation of 3 replicates. Data collection began 3 hours post GloSensor (GLOS) incubation.

Caspase-1 Consensus Sequence and pGLDEVD Specificity Probe

Upon recognizing the magnitude of an approximately ~350 fold increase in luminescence utilizing the pGLC7C1 construct from **Figure 18**, we questioned the specificity of our sensor. The short 8 amino acid sequence IQAD-SGPI present in the best performing pGLC7C1 sensor is normally present in between the p20 and p10 subunits of Pro-Caspase-7. IQAD-SGPI is known to be targeted by both Caspase-8 and 9 [89]. However, Caspase-substrate interactions are thought to also be mediated by

unidentified exosite- or protein-protein interactions between sites distal to the known region of contact or cleavage [25] [86]. This phenomenon is alleged to explain the discrepancies observed between experimentally observed *in vitro* Caspase substrates versus *in vivo* substrates [25]. The crosstalk between pyroptosis and apoptosis has been documented, and our findings are intriguing in light of these facts. However, our objective is to create a sensor specific for Caspase-1. Thus, we pursued further experiments to generate an alternative candidate sensor construct based on a well published WEHD Caspase-1 consensus cleavage sequence [71]. **Figure 20** demonstrates that we have found an alternative candidate Caspase-1 sensor in the form of a 5 amino acid WEHD insertion of a consensus sequence identified in proteomics screens.

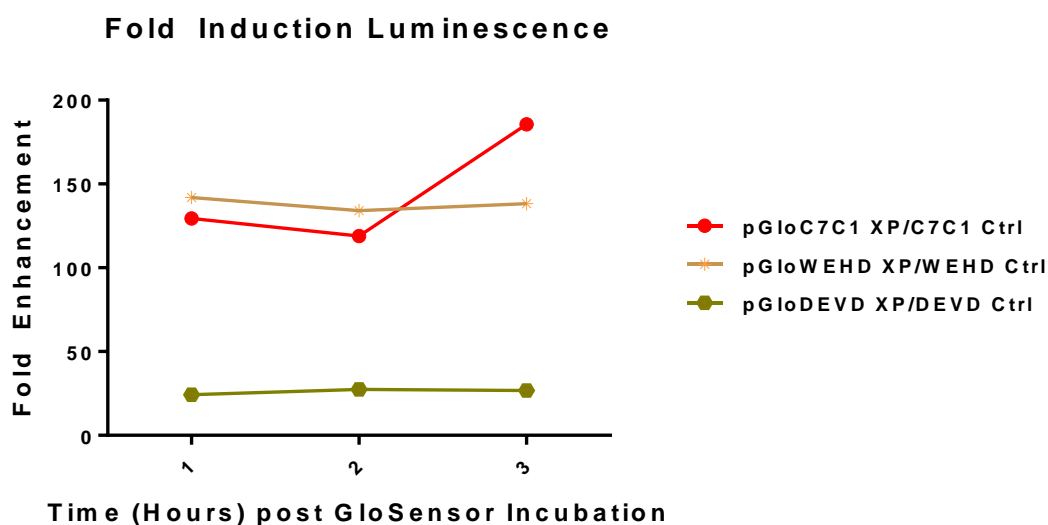


Figure 20: *Transient Transfection screen of additional Caspase 1 target constructs presented as fold induction over control values.*

Fold induction luminescence of experimental wells versus control. Values are calculated by dividing pGLO candidate XP value by pGLO candidate CTRL value at each indicated time point. Data represent the mean of 3 replicates

Generation of pLVX Vector – Molecular Cloning

Next, we probed the sensitivity of our sensor by generating two HeLa stable cell lines with a single insertion of the open reading frame encoded by pGLC7C1 and pGLIL18. To create our lentiviral vector we first needed to insert Xho1 and EcoR1 restriction sites flanking the ORF of the pGLC7C1 and pGLIL18 gene as described in the **Materials and Methods**. We double digested the MCS and the PCR amplified sensor genes themselves with Xho1 and EcoR1 respectively. The middle band shown in **Figure 21-22** corresponds to the pGLC7C1 or pGLIL18 ORF sensor gene pLVX insertion.

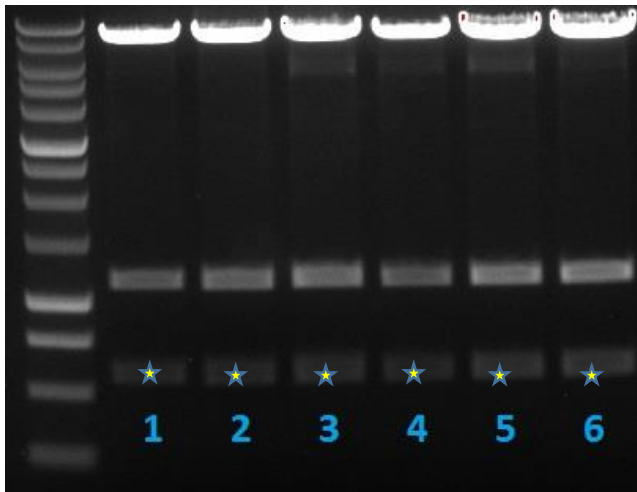


Figure 21: *pLVXC7C1 diagnostic restriction digest*

Lanes marked with a star indicate a clone positive for insertion of the pGLO ORF as verified by diagnostic digest by via Xho1 and EcoR1. The middle band of each lane is the predicted size for the pGLO ORF.

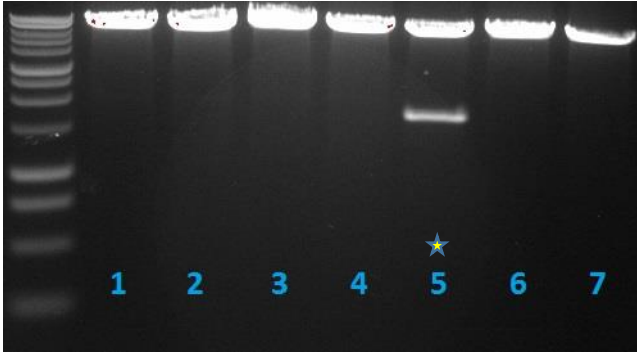


Figure 22: *pLVXIL18 diagnostic restriction digest*

Lanes marked with a star indicate a clone positive for insertion of the pGLO ORF as verified by diagnostic digest by via Xho1 and EcoR1. The middle band of each lane is the predicted size for the pGLO ORF.

Inflammasome activation in HeLa stable cell line

We generated a stable cell line, HeLa C7C1 incorporating a lentiviral insertion of our pGLC7C1 gene. Although HeLa cells are not of the myeloid lineage, we were able to induce Inflammasome activation through a Lipofectamine 2000 transfection of ASC and Pro-Caspase-1.

HeLa C7C1 cells were transfected, in triplicate, overnight and luminescence measured 14 hours post transfection in a 96 well plate. All wells were treated with GloSensor one hour before taking readings. The first group **HeLa C7C1 alone (-)** consisted of HeLa C7C1 cells treated with GloSensor only. Each control well of the group **HeLa C7C1 + GFP (Figure 23)** received 100ng GFP and .3 ul Lipofectamine 2000. Each experimental well of the group **HeLa C7C1 + ASC/Pro1 (Figure 23)**

received 50ng GFP, 25ng ASC, and 25 ng Pro-1. Time is in Hours post GloSensor (GLOS) incubation.

One can see in **Figure 23, B** that the transfection itself did not contribute to inflammasome activation. Thus all of the signal must be due to our overexpression paradigm. Fold enhancement luminescence ranged from ~14-20, a statistically significant outcome. This data shows that genomic insertion and expression of one copy of pGLC7C1 is sufficient to measure inflammasome activation in our NLRP3 over expression system. Next we set out to place pGLC7C1 under control of a stronger promoter which could then be utilized to generate a different viral vector suitable for creation of an *in vivo* animal model

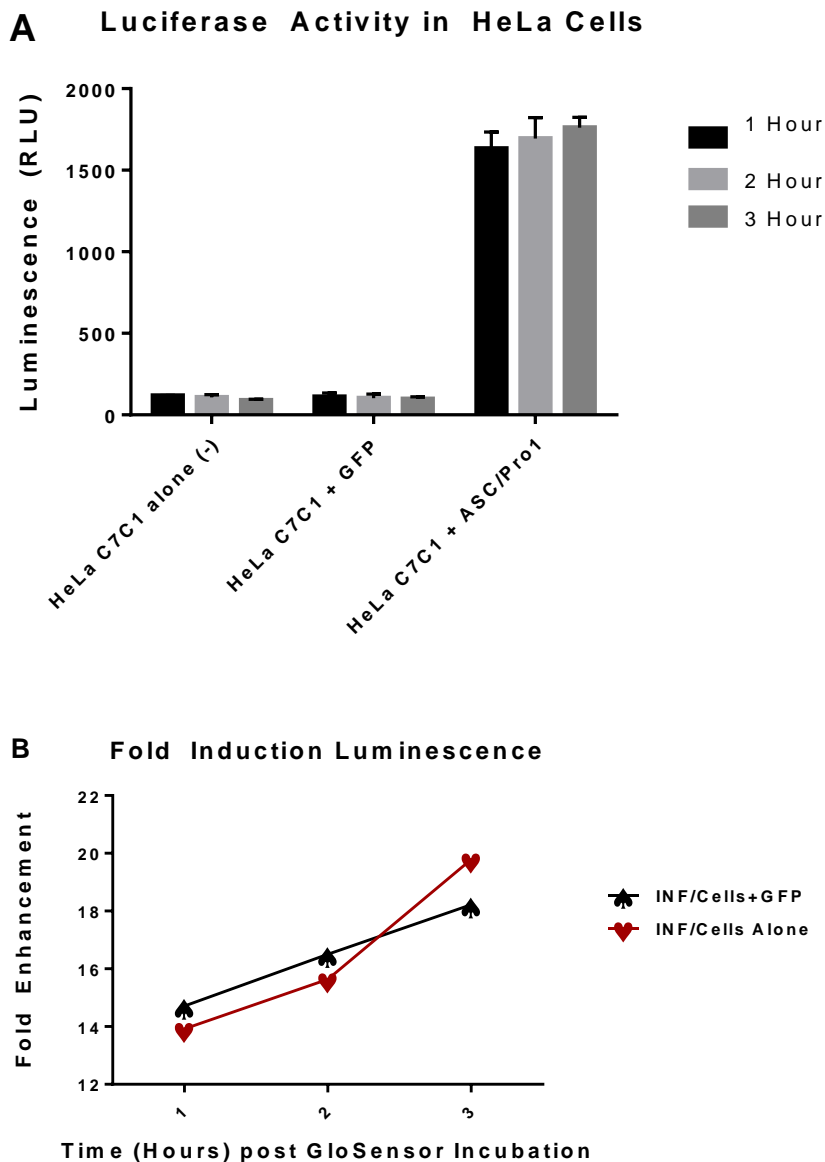


Figure 23: *HeLa stable cell line Lipofectamine 2000 transfection*

- (A) Luminometer data from Lipofectamine 2000 transfection of HeLa cells. Each respective bar indicate data gathered 1 hour (Time 1), 2 hours (Time 2), or 3 hours (Time 3) post GloSensor incubation. Data represent the mean and standard deviation of 3 replicates.
- (B) Fold induction luminescence of experimental well versus control. Values are calculated by dividing pGLO candidate XP value by pGLO candidate CTRL value at each indicated time point. Data represent the mean of 3 replicates.

Generation of pGLAAV-C7C1

Following the success of the HeLa C7C1 stable cell line experiment the next goal is creation of an *in vivo* animal model. We set forth to make an Adeno-Associated-Virus (AAV) more commonly known in the realm of gene therapy. AAV's form extrachromosomal concatamers inside the cells they infect which will stably express a gene of interest [90]. While we did not choose to move forward with utilizing the pGLAAV-MCS with the pGLC7C1 gene insertion, the evidence for successful cloning can be seen in **Figure 24**. The AAV-MCS promoter uniquely contains a β -globin intron element between the CMV promoter and MCS. Thus we utilized our HEK293T overexpression system to achieve ~43,000 RLU at a 1 and 2 hour time point with a pGLAAV-C7C1 plasmid. (**data not shown**)

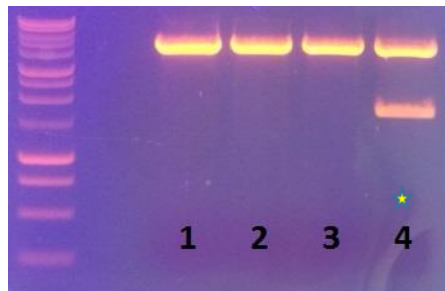


Figure 24: *pGLAAV -C7C1 diagnostic restriction digest*

Lanes marked with a star indicate a clone positive for insertion of the pGLO ORF as verified by diagnostic digest by via EcoR1 and Xho1. The middle band of each lane is the predicted size for the pGLO ORF.

Generation of pCAGC7C1, pCAG18, pCAGWE

Upon observing the large increase in luminescence with our pGLC7 sensor under control of an AAV promoter in the pAAV-MCS-C7C1 construct, we set out to place our gene under control of a different promoter. The synthetic CAG promoter consists of the CMV early enhancer, the promoter and part of the gene encoding chicken- β -actin, as well as the rabbit- β globin hybrid promoter. The CAG enhancer-promoter element can be utilized to drive very high levels of constitutive gene expression in mammals. We utilized our HEK293T overexpression system to achieve ~50,000 RLU with our pGLC7C1 sensor gene inserted into the pCAG-MCS (Multiple **(data not shown)**). We have cloned the pGLIL18, and pGLWEHD ORF into the pCAG-MCS in order to create additional transgenic mice. We hypothesize that a stable insertion of multiple copies of the pCAGC7, pCAG18, or pCAGWEHD into all of the cells of a transgenic mouse will lead to an *in vivo* animal model capable of detecting Caspase-1 activity in real time.

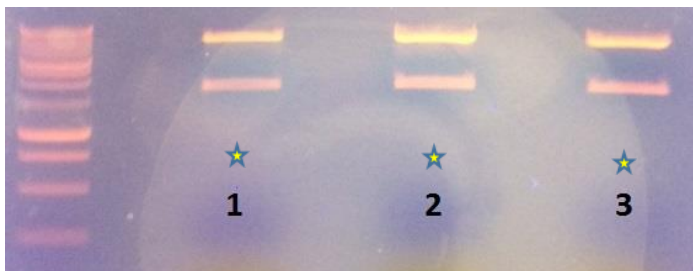


Figure 25: *pCAGC7C1* diagnostic restriction digest

Lanes marked with a star indicate a clone positive for insertion of the pGLO ORF as verified by diagnostic digest by via EcoR1 and Xho1. The middle band of each lane is the predicted size for the pGLO ORF.

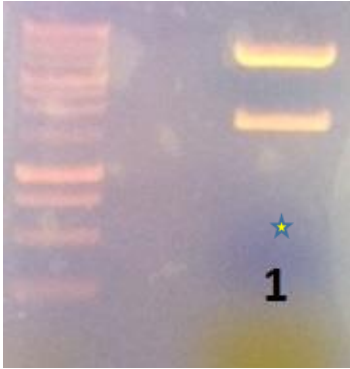


Figure 26: *pCAG-IL18 diagnostic restriction digest*

Lanes marked with a star indicate a clone positive for insertion of the pGLO ORF as verified by diagnostic digest by via EcoR1 and Xho1. The middle band of each lane is the predicted size for the pGLO ORF.

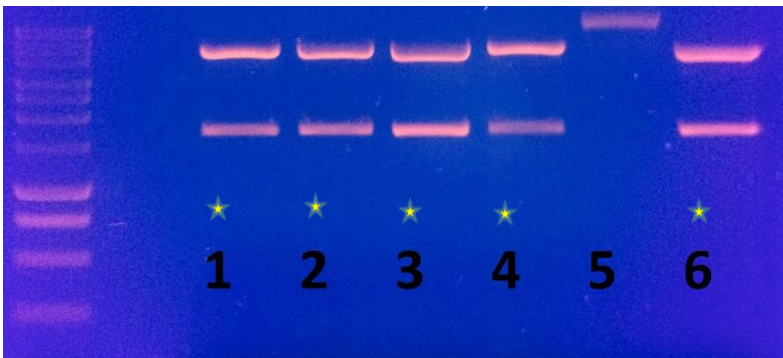


Figure 27: *pCAG-WEHD diagnostic restriction digest*

Lanes marked with a star indicate a clone positive for insertion of the pGLO ORF as verified by diagnostic digest by via EcoR1 and Xho1. The middle band of each lane is the predicted size for the pGLO ORF.

CHAPTER FOUR

DISCUSSION

The ability to quantify inflammasome activation both *in vitro* and *in vivo* with a large dynamic range and lack of significant background interference is a necessary advance to drive development of new therapeutics. The assay we have developed is not without flaws to be worked out before the potential for widespread use is realized. Our pGLO based Caspase-1 sensors must be shown to exhibit a statistically significant increase in luminescence in a myeloid cell line. Sensor activation must also be induced by a physiologically relevant stimulus such as a DAMP or PAMP.

In this study, we utilized an overexpression system in HEK293T and HeLa cell lines. We have transfected two out of three components of the NLRP3 inflammasome and observed that overexpression of ASC and Pro-Caspase-1 leads to activation of a panel of pGLO derived Caspase-1 protease sensors. The NLRP3 receptor is a known component of the NLRP3 inflammasome; thus our overexpression system may not achieve maximal inflammasome activation [31]. This is encouraging logic; leaving the door open to the potential of the sensor in a physiologically relevant setting under control of a highly active promoter. However, to counter this logic we performed an experiment in which we overexpressed the NLRC4 inflammasome components (IPAF and Pro-Caspase-1) side by side with ASC and Pro-Caspase-1 which; lead to equivalent levels of luminescence (RLU) in our pGLC7C1-HEK293T paradigm.

Overexpression of Caspase-1 has been shown to induce apoptosis, a phenomenon which we did not observe 24 hours post data collection [91].

We created a stable cell line through a pLVX vector mediated incorporation of the pGLC7C1 ORF into a non-myeloid cell line (HeLa C7C1) and induced activation of our pGLO inflammasome sensor through overexpression of ASC and Pro-Caspase-1. This data in **Figure 22**, illustrate the approximately 20-fold maximal increase in luminescence in response to overexpression of ASC and Pro-Caspase-1; NLRP3 inflammasome components in this stable cell line. It can be seen that stable insertion of one copy of our pGLC7C1 ORF via a pLVX Lentiviral vector in our HeLa C7C1 stable cell line results in a much lower fold induction luminescence as well as absolute RLU values versus the HEK293T transfection paradigm. This effect could also be due to decreased transfection efficiency of ASC and Pro-Caspase-1 in the HeLa C7C1 cells versus HEK293T. Variances in the stability of the inflammasome components in each cell line through factors such as differential gene expression of regulatory components such as POP's or COP's could play a role [41, 45].

We attempted to induce inflammasome activation in the HeLa C7C1 stable cell line through a dose response treatment of the pore forming toxin, Nigericin. We generated a BV2 C7C1 microglia stable cell line analogous to the HeLa C7C1 line. We induced inflammasome activation via a dose response treatment of a pesticide, Rotenone. These treatments failed to produce statistically significant luminescence output in our HeLa C7C1 and BV2 C7C1 microglia stable cell lines. The lack of an effect in HeLa cells may be attributed to lack of normal expression of inflammasome components.

Microglial expression of inflammasome components is documented, but the relationship between Neurological Disease and Inflammation is only beginning to be elucidated. [10, 35, 92]. One could speculate that a single insertion of the pGLC7C1 sensor gene through infection via the pLVX lentiviral vector produced insufficient levels of pGLC7C1 protein.

Next, we infected primary human monocytes and macrophages with pLVX lentiviral vector incorporating the pGLC7C1 ORF. We tested activation of the Inflammasome in response to a physiologically relevant stimulus – supernatant containing alpha-toxin from a strain of Methicillin-Resistant *Staph aureus*, MRSA courtesy of Dr. Francis Alonzo [93]. These experiments failed to detect any significant increase in luminescence in response to a known Inflammasome activator.

Maintaining physiological relevancy is important to elicit further investment in this technology. The cloning of our pGLO sensor genes downstream of strong AAV or CAG promoters will allow for increased luminescent output due to increased levels of protein expression. Under the same experimental HEK293T transfection paradigm exhibited in **(Figure 16)**, we have shown an approximate 40000-50000 (RLU) output in luminescence (RLU) with the pGLC7C1 ORF under control of an AAV or CAG synthetic promoter. It remains to be determined if a pGLO inflammasome sensor under control of the CAG or AAV promoter will elicit statistically significant increase in luminescence in response to a physiologically relevant stimulus *in vivo* or in an isolated primary cell culture system.

The specificity of the sensor is at the crux of the future utility of this assay. The best performing pGLO sensor, pGLC7C1 utilized the 8 amino acid sequence insertion belonging to Pro-Caspase-7 [86, 89]. It is possible that pGLC7C1 could detect activation of other Caspases, particularly Caspase-3/7. It is known that activation of an individual Caspases is mediated specifically by one or more other individual Caspases or the original Caspase itself. [21]. This possibility was addressed via cloning of the Caspase-1 consensus sequence WEHD into the pGLO vector. In our favor, Caspase 3 has a flap over its active site, which is absent in Caspase-1 perhaps suggesting the exclusion of certain substrates such as bulky amino acids like tryptophan, W [94, 95]. These produced similar levels of luminescence in our HEK293T paradigm illustrating two inflammasome sensors with the same sensitivity but perhaps differing specificities. A potential problem with this sensor is an overlap in P4 site specificities amongst all of the Group 1 Inflammatory Caspases. pGLWEHD may be sensitive to Caspase 1 as well as 4 and 5 and thus may prove to be a Group 1 Inflammatory Caspase sensor. If future experiments elicit a signal in response to a physiologically relevant stimulus then one would certainly want to inhibit Caspase 4, or 5, or both to test for the sensors specificity.

We have conclusively added Caspase-1 to the list of proteases able to be monitored via modifications to a Promega ® developed circularly permuted Firefly Luciferase (cpLUC). While the data documented in this thesis is encouraging, the fact of the matter is that a German group has developed an inflammasome Assay (iGLUC) based on the aforementioned *Gaussia* luciferase which catalyzes raw luminescence signals far

brighter than those capable with Firefly Luciferase [96]. *Gaussia* luciferase marketed by Promega® as Nano-Luc is fast becoming the alternative to Firefly Luciferase.

The potential to generate a stable cell line for High-Throughput-Screening of candidate therapeutics for the myriad diseases continually being found to have a component of inflammasome activity still exists. The recent Q3 release of the Promega Caspase-Glo® 1 inflammasome Assay presents an alternative to our assay if we choose to pivot towards a HTS approach. Promega® product supporting data indicates that the Caspase-Glo® 1 assay can reach ~22,000 RLU in treated Pam3CSK4 cells in addition to the ability to monitor Caspase-1 activity in the culture medium. However, a poor signal to noise ratio of 12.40 in culture media or 4.63 in Pam3CSK4 cells indicate the lack of a broad dynamic range. A final test of the utility of pGLO in serving as a sensor of the inflammasome in an HTS setting would surely involve lentiviral or other viral mediated stable insertion of a pGLO sensor gene under control of the highly active CAG promoter. This could present an inexpensive alternative to the Caspase-Glo® 1 assay as one can use the Luciferin reagents from the Dual-Luciferase assay for a lytic end-point assay as an alternative to the cAMP gloSensor (GLOS) reagent mediated ability to take readings over the course of hours. Prior to performing this test it would be important to perform another HTS screen through error-prone-PCR or one of many various mutagenic methods to generate the sensor with the best possible catalytic activity.

The scientific impact of the successful directed evolution of a natural protein to serve as a sensor for myriad proteases by Promega®, in live cells over time is substantial [27]. The utility in the pGLO system is in the ability to sense a protease possessing an

exposed active site, like the Caspase family, with little dependence on exosites for their catalytic activity [25]. The data documented in this thesis should not discourage one from pursuing development of a custom protease sensor for a protease of interest via the pGLO system [9, 19, 23, 27, 84]. Caspase-1 is known to be quickly and transiently activated; followed by rapid deactivation in a wild-type scenario as opposed to apoptotic Caspase 3/7 [97]. The existence of databases such as CutDB (cutdb.burnham.org) - which *extensively* document proteases and their cleavage sites sets the stage for a new generation of sensors which depart from the more conservative, highly cited consensus cleavage sequences like DEVD, or WEHD, and into natural substrates such as IQAD-SGPI present in the Caspase 7 zymogen.

BIBLIOGRAPHY

1. Medzhitov, R., *Origin and physiological roles of inflammation*. Nature, 2008. **454**(7203): p. 428-35.
2. Schroder, K. and J. Tschopp, *The inflammasomes*. Cell, 2010. **140**(6): p. 821-32.
3. Martinon, F., K. Burns, and J. Tschopp, *The inflammasome: a molecular platform triggering activation of inflammatory caspases and processing of proIL-beta*. Mol Cell, 2002. **10**(2): p. 417-26.
4. Strowig, T., et al., *Inflammasomes in health and disease*. Nature, 2012. **481**(7381): p. 278-86.
5. Masters, S.L., *Specific inflammasomes in complex diseases*. Clin Immunol, 2013. **147**(3): p. 223-8.
6. Volin, M.V. and A.E. Koch, *Interleukin-18: a mediator of inflammation and angiogenesis in rheumatoid arthritis*. J Interferon Cytokine Res, 2011. **31**(10): p. 745-51.
7. Martinon, F., et al., *Gout-associated uric acid crystals activate the NALP3 inflammasome*. Nature, 2006. **440**(7081): p. 237-41.
8. Codolo, G., et al., *Triggering of inflammasome by aggregated alpha-synuclein, an inflammatory response in synucleinopathies*. PLoS One, 2013. **8**(1): p. e55375.
9. Wigdal, S.S., et al., *A novel bioluminescent protease assay using engineered firefly luciferase*. Curr Chem Genomics, 2008. **2**: p. 16-28.
10. Walsh, J.G., D.A. Muruve, and C. Power, *Inflammasomes in the CNS*. Nat Rev Neurosci, 2014. **15**(2): p. 84-97.
11. Halle, A., et al., *The NALP3 inflammasome is involved in the innate immune response to amyloid-beta*. Nat Immunol, 2008. **9**(8): p. 857-65.
12. Burns, A. and S. Iliffe, *Alzheimer's disease*. BMJ, 2009. **338**: p. b158.
13. de Zoete, M.R., et al., *Inflammasomes*. Cold Spring Harb Perspect Biol, 2014. **6**(12): p. a016287.

14. Martinon, F., A. Mayor, and J. Tschopp, *The inflammasomes: guardians of the body*. *Annu Rev Immunol*, 2009. **27**: p. 229-65.
15. Latz, E., *The inflammasomes: mechanisms of activation and function*. *Curr Opin Immunol*, 2010. **22**(1): p. 28-33.
16. Karmakar, M., et al., *Neutrophil IL-1beta processing induced by pneumolysin is mediated by the NLRP3/ASC inflammasome and caspase-1 activation and is dependent on K+ efflux*. *J Immunol*, 2015. **194**(4): p. 1763-75.
17. Broz, P. and D.M. Monack, *Measuring inflammasome activation in response to bacterial infection*. *Methods Mol Biol*, 2013. **1040**: p. 65-84.
18. Gross, O., *Measuring the inflammasome*. *Methods Mol Biol*, 2012. **844**: p. 199-222.
19. Fan, F., et al., *Novel genetically encoded biosensors using firefly luciferase*. *ACS Chem Biol*, 2008. **3**(6): p. 346-51.
20. Fan, F. and K.V. Wood, *Bioluminescent assays for high-throughput screening*. *Assay Drug Dev Technol*, 2007. **5**(1): p. 127-36.
21. Earnshaw, W.C., L.M. Martins, and S.H. Kaufmann, *Mammalian caspases: structure, activation, substrates, and functions during apoptosis*. *Annu Rev Biochem*, 1999. **68**: p. 383-424.
22. Conti, E., N.P. Franks, and P. Brick, *Crystal structure of firefly luciferase throws light on a superfamily of adenylate-forming enzymes*. *Structure*, 1996. **4**(3): p. 287-98.
23. Binkowski, B.F., et al., *A luminescent biosensor with increased dynamic range for intracellular cAMP*. *ACS Chem Biol*, 2011. **6**(11): p. 1193-7.
24. Binkowski, B.F., F. Fan, and K.V. Wood, *Luminescent biosensors for real-time monitoring of intracellular cAMP*. *Methods Mol Biol*, 2011. **756**: p. 263-71.
25. Timmer, J.C. and G.S. Salvesen, *Caspase substrates*. *Cell Death Differ*, 2007. **14**(1): p. 66-72.
26. Lopez-Otin, C. and L.M. Matrisian, *Emerging roles of proteases in tumour suppression*. *Nat Rev Cancer*, 2007. **7**(10): p. 800-8.
27. Galban, S., et al., *Imaging proteolytic activity in live cells and animal models*. *PLoS One*, 2013. **8**(6): p. e66248.
28. Vanbervliet, B., et al., *The inducible CXCR3 ligands control plasmacytoid dendritic cell responsiveness to the constitutive chemokine stromal cell-derived factor 1 (SDF-1)/CXCL12*. *J Exp Med*, 2003. **198**(5): p. 823-30.

29. Cavaillon, J.M., *Cytokines and macrophages*. Biomed Pharmacother, 1994. **48**(10): p. 445-53.
30. Martinon, F. and J. Tschopp, *Inflammatory caspases: linking an intracellular innate immune system to autoinflammatory diseases*. Cell, 2004. **117**(5): p. 561-74.
31. Bell, J.K., et al., *Leucine-rich repeats and pathogen recognition in Toll-like receptors*. Trends Immunol, 2003. **24**(10): p. 528-33.
32. Crawford, E.D. and J.A. Wells, *Caspase substrates and cellular remodeling*. Annu Rev Biochem, 2011. **80**: p. 1055-87.
33. Vollmer, J., et al., *Characterization of three CpG oligodeoxynucleotide classes with distinct immunostimulatory activities*. Eur J Immunol, 2004. **34**(1): p. 251-62.
34. Tsujimoto, Y., *Role of Bcl-2 family proteins in apoptosis: apoptosomes or mitochondria?* Genes Cells, 1998. **3**(11): p. 697-707.
35. Liu, S.B., W.L. Mi, and Y.Q. Wang, *Research progress on the NLRP3 inflammasome and its role in the central nervous system*. Neurosci Bull, 2013. **29**(6): p. 779-87.
36. Mariathasan, S., et al., *Differential activation of the inflammasome by caspase-1 adaptors ASC and Ipaf*. Nature, 2004. **430**(6996): p. 213-8.
37. Faustin, B., et al., *Reconstituted NALP1 inflammasome reveals two-step mechanism of caspase-1 activation*. Mol Cell, 2007. **25**(5): p. 713-24.
38. Franchi, L., et al., *Intracellular NOD-like receptors in innate immunity, infection and disease*. Cell Microbiol, 2008. **10**(1): p. 1-8.
39. Martinon, F., *Orchestration of pathogen recognition by inflammasome diversity: Variations on a common theme*. Eur J Immunol, 2007. **37**(11): p. 3003-6.
40. Miao, E.A., J.V. Rajan, and A. Aderem, *Caspase-1-induced pyroptotic cell death*. Immunol Rev, 2011. **243**(1): p. 206-14.
41. Stehlik, C. and A. Dorfleutner, *COPs and POPs: modulators of inflammasome activity*. J Immunol, 2007. **179**(12): p. 7993-8.
42. Bryan, N.B., et al., *Activation of inflammasomes requires intracellular redistribution of the apoptotic speck-like protein containing a caspase recruitment domain*. J Immunol, 2009. **182**(5): p. 3173-82.

43. Bryan, N.B., et al., *Differential splicing of the apoptosis-associated speck like protein containing a caspase recruitment domain (ASC) regulates inflammasomes*. J Inflamm (Lond), 2010. **7**: p. 23.
44. Bourke, E., et al., *IL-1 beta scavenging by the type II IL-1 decoy receptor in human neutrophils*. J Immunol, 2003. **170**(12): p. 5999-6005.
45. Latz, E., T.S. Xiao, and A. Stutz, *Activation and regulation of the inflammasomes*. Nat Rev Immunol, 2013. **13**(6): p. 397-411.
46. Krishnaswamy, J.K., D. Liu, and S.C. Eisenbarth, *POP goes the inflammasome*. Nat Immunol, 2014. **15**(4): p. 311-3.
47. Johnston, J.B., et al., *A poxvirus-encoded pyrin domain protein interacts with ASC-1 to inhibit host inflammatory and apoptotic responses to infection*. Immunity, 2005. **23**(6): p. 587-98.
48. Lee, S.H., C. Stehlik, and J.C. Reed, *Cop, a caspase recruitment domain-containing protein and inhibitor of caspase-1 activation processing*. J Biol Chem, 2001. **276**(37): p. 34495-500.
49. Druilhe, A., et al., *Regulation of IL-1beta generation by Pseudo-ICE and ICEBERG, two dominant negative caspase recruitment domain proteins*. Cell Death Differ, 2001. **8**(6): p. 649-57.
50. Guarda, G., et al., *Type I interferon inhibits interleukin-1 production and inflammasome activation*. Immunity, 2011. **34**(2): p. 213-23.
51. Freeman, D., et al., *Alpha-synuclein induces lysosomal rupture and cathepsin dependent reactive oxygen species following endocytosis*. PLoS One, 2013. **8**(4): p. e62143.
52. Hornung, V., et al., *Silica crystals and aluminum salts activate the NALP3 inflammasome through phagosomal destabilization*. Nat Immunol, 2008. **9**(8): p. 847-56.
53. Petrilli, V., et al., *Activation of the NALP3 inflammasome is triggered by low intracellular potassium concentration*. Cell Death Differ, 2007. **14**(9): p. 1583-9.
54. Kanneganti, T.D., et al., *Pannexin-1-mediated recognition of bacterial molecules activates the cryopyrin inflammasome independent of Toll-like receptor signaling*. Immunity, 2007. **26**(4): p. 433-43.
55. Zhou, R., et al., *Thioredoxin-interacting protein links oxidative stress to inflammasome activation*. Nat Immunol, 2010. **11**(2): p. 136-40.
56. Haneklaus, M., L.A. O'Neill, and R.C. Coll, *Modulatory mechanisms controlling the NLRP3 inflammasome in inflammation: recent developments*. Curr Opin Immunol, 2013. **25**(1): p. 40-5.

57. Chen, C.Z., et al., *MicroRNAs modulate hematopoietic lineage differentiation*. Science, 2004. **303**(5654): p. 83-6.
58. Juliana, C., et al., *Non-transcriptional priming and deubiquitination regulate NLRP3 inflammasome activation*. J Biol Chem, 2012. **287**(43): p. 36617-22.
59. Lu, B., et al., *Novel role of PKR in inflammasome activation and HMGB1 release*. Nature, 2012. **488**(7413): p. 670-4.
60. Mayor, A., et al., *A crucial function of SGT1 and HSP90 in inflammasome activity links mammalian and plant innate immune responses*. Nat Immunol, 2007. **8**(5): p. 497-503.
61. Zhou, R., et al., *A role for mitochondria in NLRP3 inflammasome activation*. Nature, 2011. **469**(7329): p. 221-5.
62. Nakahira, K., et al., *Autophagy proteins regulate innate immune responses by inhibiting the release of mitochondrial DNA mediated by the NALP3 inflammasome*. Nat Immunol, 2011. **12**(3): p. 222-30.
63. Meissner, F., K. Molawi, and A. Zychlinsky, *Superoxide dismutase 1 regulates caspase-1 and endotoxic shock*. Nat Immunol, 2008. **9**(8): p. 866-72.
64. Jha, S., et al., *The inflammasome sensor, NLRP3, regulates CNS inflammation and demyelination via caspase-1 and interleukin-18*. J Neurosci, 2010. **30**(47): p. 15811-20.
65. Chakraborty, S., et al., *Inflammasome signaling at the heart of central nervous system pathology*. J Neurosci Res, 2010. **88**(8): p. 1615-31.
66. Larsen, C.M., et al., *Sustained effects of interleukin-1 receptor antagonist treatment in type 2 diabetes*. Diabetes Care, 2009. **32**(9): p. 1663-8.
67. Larsen, C.M., et al., *Interleukin-1-receptor antagonist in type 2 diabetes mellitus*. N Engl J Med, 2007. **356**(15): p. 1517-26.
68. Masters, S.L., et al., *Activation of the NLRP3 inflammasome by islet amyloid polypeptide provides a mechanism for enhanced IL-1beta in type 2 diabetes*. Nat Immunol, 2010. **11**(10): p. 897-904.
69. Boni-Schnetzler, M. and M.Y. Donath, *How biologics targeting the IL-1 system are being considered for the treatment of type 2 diabetes*. Br J Clin Pharmacol, 2013. **76**(2): p. 263-8.
70. Thornberry, N.A., et al., *A combinatorial approach defines specificities of members of the caspase family and granzyme B. Functional relationships established for key mediators of apoptosis*. J Biol Chem, 1997. **272**(29): p. 17907-11.
71. Li, J. and J. Yuan, *Caspases in apoptosis and beyond*. Oncogene, 2008. **27**(48): p. 6194-206.

- 72 .Sollberger, G., et al., *Caspase-1: the inflammasome and beyond*. *Innate Immun*, 2014. **20**(2): p. 115-25.
- 73 .Greer, L.F., 3rd and A.A. Szalay, *Imaging of light emission from the expression of luciferases in living cells and organisms: a review*. *Luminescence*, 2002. **17**(1): p. 43-74.
- 74 .Thorne, N., J. Inglese, and D.S. Auld, *Illuminating insights into firefly luciferase and other bioluminescent reporters used in chemical biology*. *Chem Biol*, 2010. **17**(6): p. 646-57.
75. Maguire, C.A., et al., *Gaussia luciferase variant for high-throughput functional screening applications*. *Anal Chem*, 2009. **81**(16): p. 7102-6.
- 76 .de Wet, J.R., et al., *Cloning of firefly luciferase cDNA and the expression of active luciferase in Escherichia coli*. *Proc Natl Acad Sci U S A*, 1985. **82**(23): p. 7870-3.
77. Fujii, H., et al., *Increase in bioluminescence intensity of firefly luciferase using genetic modification*. *Anal Biochem*, 2007. **366**(2): p. 131-6.
78. Baird, G.S., D.A. Zacharias, and R.Y. Tsien, *Circular permutation and receptor insertion within green fluorescent proteins*. *Proc Natl Acad Sci U S A*, 1999. **96**(20): p. 11241-6.
79. Yu, Y. and S. Lutz, *Circular permutation: a different way to engineer enzyme structure and function*. *Trends Biotechnol*, 2011. **29**(1): p. 18-25.
- 80 .Ozawa, T., et al., *Split luciferase as an optical probe for detecting protein-protein interactions in mammalian cells based on protein splicing*. *Anal Chem*, 2001. **73**(11): p. 2516-21.
- 81 .Coppola, J.M., B.D. Ross, and A. Rehemtulla, *Noninvasive imaging of apoptosis and its application in cancer therapeutics*. *Clin Cancer Res*, 2008. **14**(8): p. 2492-501.
- 82 .Kilianski, A., et al., *Assessing activity and inhibition of Middle East respiratory syndrome coronavirus papain-like and 3C-like proteases using luciferase-based biosensors*. *J Virol*, 2013. **87**(21): p. 11955-62.
83. Vrazo, A.C., et al., *Live cell evaluation of granzyme delivery and death receptor signaling in tumor cells targeted by human natural killer cells*. *Blood*, 2015.
- 84 .Li, J., et al., *Real-time detection of CTL function reveals distinct patterns of caspase activation mediated by Fas versus granzyme B*. *J Immunol*, 2014. **193**(2): p. 519-28.
85. Kahns, S., et al., *Caspase-mediated parkin cleavage in apoptotic cell death*. *J Biol Chem*, 2002. **277**(18): p. 15303-8.
86. Lamkanfi, M., et al., *Targeted peptidecentric proteomics reveals caspase-7 as a substrate of the caspase-1 inflammasomes*. *Mol Cell Proteomics*, 2008. **7**(12): p. 2350-63.

- 87 .Howard, A.D., et al., *IL-1-converting enzyme requires aspartic acid residues for processing of the IL-1 beta precursor at two distinct sites and does not cleave 31-kDa IL-1 alpha*. J Immunol, 1991. **147**(9): p. 2964-9.
- 88 .Akita, K., et al., *Involvement of caspase-1 and caspase-3 in the production and processing of mature human interleukin 18 in monocytic THP.1 cells*. J Biol Chem, 1997. **272**(42): p. 26595-603.
- 89 .Chai, J., et al., *Crystal structure of a procaspase-7 zymogen: mechanisms of activation and substrate binding*. Cell, 2001. **107**(3): p. 399-407.
- 90 .Nakai, H., et al., *Free DNA ends are essential for concatemerization of synthetic double-stranded adeno-associated virus vector genomes transfected into mouse hepatocytes in vivo*. Mol Ther, 2003. **7**(1): p. 112-21.
- 91 .Miura, M., et al., *Induction of apoptosis in fibroblasts by IL-1 beta-converting enzyme, a mammalian homolog of the C. elegans cell death gene ced-3*. Cell, 1993. **75**(4): p. 653-60.
92. Walsh, J.G., et al., *Rapid inflammasome activation in microglia contributes to brain disease in HIV/AIDS*. Retrovirology, 2014. **11**: p. 35.
93. Craven, R.R., et al., *Staphylococcus aureus alpha-hemolysin activates the NLRP3-inflammasome in human and mouse monocytic cells*. PLoS One, 2009. **4**(10): p. e7446.
94. Rotonda, J., et al., *The three-dimensional structure of apopain/CPP32, a key mediator of apoptosis*. Nat Struct Biol, 1996. **3**(7): p. 619-25.
95. Mittl, P.R., et al., *Structure of recombinant human CPP32 in complex with the tetrapeptide acetyl-Asp-Val-Ala-Asp fluoromethyl ketone*. J Biol Chem, 1997. **272**(10): p. 6539-47.
96. Bartok, E., et al., *iGLuc: a luciferase-based inflammasome and protease activity reporter*. Nat Methods, 2013. **10**(2): p. 147-54.
97. Walsh, J.G., et al., *Caspase-1 promiscuity is counterbalanced by rapid inactivation of processed enzyme*. J Biol Chem, 2011. **286**(37): p. 32513-24.

VITA

Michael Alexander Winek was born in Hinsdale, IL. He completed his secondary education at Neuqua Valley High School and continued his studies at University of Iowa where he earned a Bachelor of Science in Neurobiology. After graduation he was employed at LabCorp as a Support Services Team Lead in Elmhurst, IL.

In the fall of 2013, Michael entered the Neuroscience Graduate Program as an MS student at Loyola University Chicago. He joined the laboratory of Dr. Edward Campbell where he began investigating the development of a bioluminescence sensor of Inflammasome activation. Michael will be continuing his work in the biomedical sciences for Invenra, Inc in Madison WI.